

The Minimal Flavour Violation benchmark in view of the latest LHCb data

Tobias Hurth¹

*Institute for Physics, Johannes Gutenberg University,
D-55099 Mainz, Germany*

Farvah Mahmoudi²

*CERN Theory Division, Physics Department,
CH-1211 Geneva 23, Switzerland
Clermont Université, Université Blaise Pascal, CNRS/IN2P3,
LPC, BP 10448, 63000 Clermont-Ferrand, France*

Abstract: We derive the consequences of the MFV hypothesis for $\Delta F = 1$ flavour observables based on the latest LHCb data. Any future measurements beyond the MFV bounds and relations unambiguously indicate the existence of new flavour structures next to the Yukawa couplings of the Standard Model.

¹Email: tobias.hurth@cern.ch

²Email: mahmoudi@in2p3.fr

1 Introduction

The last decade of quark flavour experiments has shown an impressive success of the simple CKM mechanism for flavour mixing and CP violation: All measurements of rare decays ($\Delta F = 1$), of mixing phenomena ($\Delta F = 2$), and of all CP violating observables at tree and loop level have been consistent with the Cabibbo-Kobayashi-Maskawa (CKM) theory of the Standard Model (SM); in other words none of the former and present flavour experiments including the first generation of the B factories at KEK (Belle experiment at the KEKB e^+e^- collider) [1] and at SLAC (BaBar experiment at the PEP-II e^+e^- collider) [2], and the Tevatron B physics programs (CDF [3] and D0 [4] experiments) has found an unambiguous sign of New Physics (NP). Moreover, all first results based on the high statistics of the LHCb experiment [5] are again very well in agreement with the CKM theory of the SM. Of course there have been and there are still so-called tensions, anomalies, or puzzles in the quark flavour data at 1-,2-, or 3- σ level, however, until now they all have disappeared after some time when more statistics had been collected.

This means that flavour-violating processes between quarks are governed by a 3×3 unitarity matrix referred to as the CKM matrix [6, 7]. In particular, the one phase among the four real independent parameters of the CKM matrix represents the dominating source of CP violation and it allows for a unified description of all the CP violating phenomena in the SM. This success of the CKM theory of CP violation was honored with the Nobel Prize in Physics in 2008.

This feature is somehow unexpected because in principle (loop-induced) flavour changing neutral current (FCNC) processes like $\bar{B} \rightarrow X_s \gamma$ offer high sensitivity to NP; additional contributions to the decay rate, in which SM particles are replaced by new particles such as the supersymmetric charginos or gluinos, are not suppressed by the factor $\alpha/4\pi$ relative to the SM contribution. Thus, FCNC decays provide information about the SM and its extensions via virtual effects to scales presently not accessible (for reviews see Refs. [8, 9]). This is complementary to the direct production of new particles at collider experiments [10, 11]

Within this indirect search for NP there is a an ambiguity of the NP scale. In the model-independent approach using the effective electroweak hamiltonian, the contribution to one specific operator \mathcal{O}_i can be parametrized via $(C_{\text{SM}}^i / M_W + C_{\text{NP}}^i / \Lambda_{\text{NP}}) \times \mathcal{O}_i$ where the first term represents the SM contribution at the electroweak scale M_W and the second one the NP contribution with an unknown coupling C_{SM}^i and an unknown NP scale Λ_{NP} . The non-existence of large NP effects in FCNC observables in general implies the infamous flavour problem, namely why FCNC are suppressed: Either the mass scale of the new degrees of freedom Λ_{NP} is very high or the new flavour-violating couplings C_{NP}^i are small for (symmetry?) reasons that remain to be found. For example, assuming *generic* new flavour-violating couplings of $O(1)$, the present data on K - \bar{K} mixing implies a very high NP scale of order 10^3 – 10^4 TeV depending on whether the new contributions enter at loop- or at tree-level. In contrast, theoretical considerations on the Higgs sector, which is responsible for the mass generation of the fundamental particles in the SM, call for NP at order 1 TeV. As a consequence, any NP below the 1 TeV scale must have a non-generic flavour structure.

The hypothesis of minimal flavour violation (MFV) [12–14], is a formal model-independent solution to the NP flavour problem. It assumes that the flavour and the CP symmetry are broken as in the SM. Thus, it requires that all flavour- and CP-violating interactions be linked to the known structure of Yukawa couplings. A renormalization-group invariant definition of MFV based on a symmetry principle is given in Ref. [14]; this is mandatory for a consistent effective field theoretical analysis of NP effects.

The MFV hypothesis is far from being verified. There is still room for sizable new effects, and new flavour structures beyond the Yukawa couplings are still compatible with the present data because the flavour sector has been tested only at the 10% level especially in the $b \rightarrow s$ transitions. However,

the MFV hypothesis represents an important benchmark in the sense that any measurement which is inconsistent with the general constraints and relations induced by the MFV hypothesis unambiguously indicates the existence of new flavour structures.

This implies the main purpose of the present paper, namely to derive the consequences of the MFV hypothesis based on the latest LHCb data. This was done some time ago in Ref. [15] for $\Delta F = 1$ observables. In particular the impressive start of the LHCb experiment suggests to update this analysis.

Besides the new data from the B factories and from the LHCb experiment we implement some additional theoretical improvements compared to the previous analysis of $\Delta F = 1$ processes: The exclusive $B \rightarrow K^* \ell^+ \ell^-$ decay was analyzed within a simple form factor analysis. Here we use the up-to-date theoretical tools of QCD-improved factorization for the low- q^2 region [16,17] and the recently proposed OPE methods for the high- q^2 region [18,19]. Secondly, we skip the approximation that the NP contributions to the electromagnetic and chromomagnetic operators appear in a fixed linear combination which was necessary in the previous analysis due to the limited number of independent experimental measurements.

The MFV analysis of $\Delta F = 2$ mixing phenomena decouples from the $\Delta F = 1$ analysis within the standard MFV framework. The $\Delta F = 2$ analysis in Ref. [20] was recently updated in Refs. [21,22].

The paper is organized as follows: In Section 2 we recall the definition of the RG invariant definition of the MFV hypothesis and in particular the effective hamiltonian within this framework. In Section 3 we work out the dependence on the non-standard Wilson coefficients of the MFV effective theory for all the flavour observables used in our analysis. We also discuss the various sources of the uncertainties in the theoretical predictions. In Section 4 we give some numerical details and in Section 5 we discuss our results.

2 Effective hamiltonian with MFV

2.1 MFV hypothesis

The SM gauge interactions are universal in quark flavour space, this means the gauge sector of the SM is invariant under the flavour group G_{flavour} which can be decomposed as

$$G_{\text{flavour}} = U(3)_{Q_L} \times U(3)_{U_R} \times U(3)_{D_R}. \quad (2.1)$$

In the SM this symmetry is only broken by the Yukawa couplings. Any new physics model in which all flavour- and CP-violating interactions can be linked to the known Yukawa couplings is *minimal flavour violating*. In order to implement this principle in a renormalization group invariant way [14], one promotes G_{flavour} to a symmetry of the theory by introducing auxiliary fields Y_U and Y_D transforming under $SU(3)_q^3$ as

$$Y_U (3, \bar{3}, 1) \text{ and } Y_D (3, 1, \bar{3}). \quad (2.2)$$

The Yukawa couplings are then introduced as background fields of these so-called spurions transforming under the flavour group. An effective theory satisfies the criterion of MFV if all higher-dimensional, constructed from SM and Y fields, are invariant under CP and under the flavour group G_{flavour} [14].

In the construction of the effective field theory, operators with arbitrary powers of the dimensionless $Y_{U/D}$ have to be considered in principle. However, the specific structure of the SM, with its hierarchy of CKM matrix elements and quark masses, drastically reduces the number of numerically relevant operators. For example, it can be shown that in MFV models with one Higgs doublet, all

FCNC processes with external d -type quarks are governed by the following combination of spurions due to the dominance of the top Yukawa coupling y_t :

$$(Y_U Y_U^\dagger)_{ij} \approx y_t^2 V_{3i}^* V_{3j}, \quad (2.3)$$

where a basis is used in which the d -type quark Yukawa is diagonal.

There are two strict predictions in this general class of models which have to be tested. First, the MFV hypothesis implies the usual CKM relations between $b \rightarrow s$, $b \rightarrow d$, and $s \rightarrow d$ transitions. For example, this relation allows for upper bounds on NP effects in $\text{BR}(\bar{B} \rightarrow X_d \gamma)$, and $\text{BR}(\bar{B} \rightarrow X_s \nu \bar{\nu})$ using experimental data or bounds from $\text{BR}(\bar{B} \rightarrow X_s \gamma)$, and $\text{BR}(K \rightarrow \pi^+ \nu \bar{\nu})$, respectively. This emphasizes the need for high-precision measurements of $b \rightarrow s/d$, but also of $s \rightarrow d$ transitions such as the rare kaon decay $K \rightarrow \pi \nu \bar{\nu}$.

The second prediction is that the CKM phase is the only source of CP violation. This implies that any phase measurement as in $B \rightarrow \phi K_s$ or $\Delta M_{B(s/d)}$ is not sensitive to new physics. This is an additional assumption because the breaking of the flavour group and the discrete CP symmetry is in principle not connected at all. For example there is also a renormalization-group invariant extension of the MFV concept allowing for flavour-blind phases as was shown in Ref. [45]; however these lead to non-trivial CP effects, which get strongly constrained by flavour-diagonal observables such as electric dipole moments [45]. So within the model-independent effective field theory approach of MFV we keep the minimality condition regarding CP. But in specific models like MSSM the discussion of additional CP phases within the MFV framework makes sense and can also allow for a natural solution of the well-known supersymmetric CP problem, see for example Refs. [23, 24].

Scenarios with two Higgs doublets with large $\tan \beta = O(m_t/m_b)$ allow for the unification of top and bottom Yukawa couplings as predicted in grand-unified models and for sizable new effects in helicity-suppressed decay models. There are more general MFV relations existing in this scenario due to the dominant role of scalar operators. However, since $\tan \beta$ is large, there is a new combination of spurions numerically relevant in the construction of higher-order MFV effective operators, namely

$$(Y_D Y_D^\dagger)_{ij} \approx y_d^2 \delta_{ij}, \quad (2.4)$$

which invalidates the general MFV relation between $b \rightarrow s/d$ and $s \rightarrow d$ transitions.

For more details we refer to the very recent complete mini-review on MFV [32]. Here we only add two issues on the application of the MFV hypothesis to the minimal supersymmetric standard model (MSSM). Most interestingly, the MFV hypothesis can serve as a substitute for R-parity in the MSSM [33, 34]. MFV is sufficient to forbid a too fast proton decay because when the MFV hypothesis is applied to R-parity violating terms, the spurion expansion leads to a suppression by neutrino masses and light-charged fermion masses, in this sense MFV within the MSSM can be regarded a natural theory for R-parity violation. Secondly, the MFV framework is renormalization-group invariant by construction, however, it is not clear that the hierarchy between the spurion terms is preserved when running down from the high scale to the low electroweak scale. Without this conservation of hierarchy, the MFV hypothesis would lose its practicability. However, as explicitly shown in Refs. [30, 31], a MFV-compatible change of the boundary conditions at the high scale has barely any influence on the low-scale spectrum. Finally, the MFV hypothesis solves the NP flavour problem only formally. One still has to find explicit dynamical structures to realize the MFV hypothesis like gauge-mediated supersymmetric theories. And of course the MFV hypothesis is not a theory of flavour; it does not explain the hierarchical structure of the CKM matrix and the large mass splittings of the SM fermions.

2.2 Effective hamiltonian

Our analysis is based on the following MFV effective hamiltonian relevant to $b \rightarrow s$ transitions (and also for $b \rightarrow d$ transitions with obvious replacements) [14]:

$$\begin{aligned} \mathcal{H}_{\text{eff}}^{b \rightarrow s} = & -\frac{4G_F}{\sqrt{2}} [V_{us}^* V_{ub} (C_1^c P_1^u + C_2^c P_2^u) + V_{cs}^* V_{cb} (C_1^c P_1^c + C_2^c P_2^c)] \\ & - \frac{4G_F}{\sqrt{2}} \sum_{i=3}^{10} [(V_{us}^* V_{ub} + V_{cs}^* V_{cb}) C_i^c + V_{ts}^* V_{tb} C_i^t] P_i + V_{ts}^* V_{tb} C_0^\ell P_0^\ell + \text{h.c.} \end{aligned} \quad (2.5)$$

with

$$\begin{aligned} P_1^u &= (\bar{s}_L \gamma_\mu T^a u_L) (\bar{u}_L \gamma^\mu T^a b_L), \quad P_5 = (\bar{s}_L \gamma_{\mu_1} \gamma_{\mu_2} \gamma_{\mu_3} b_L) \sum_q (\bar{q} \gamma^{\mu_1} \gamma^{\mu_2} \gamma^{\mu_3} q), \\ P_2^u &= (\bar{s}_L \gamma_\mu u_L) (\bar{u}_L \gamma^\mu b_L), \quad P_6 = (\bar{s}_L \gamma_{\mu_1} \gamma_{\mu_2} \gamma_{\mu_3} T^a b_L) \sum_q (\bar{q} \gamma^{\mu_1} \gamma^{\mu_2} \gamma^{\mu_3} T^a q), \\ P_1^c &= (\bar{s}_L \gamma_\mu T^a c_L) (\bar{c}_L \gamma^\mu T^a b_L), \quad P_7 = \frac{e}{16\pi^2} m_b (\bar{s}_L \sigma^{\mu\nu} b_R) F_{\mu\nu}, \\ P_2^c &= (\bar{s}_L \gamma_\mu c_L) (\bar{c}_L \gamma^\mu b_L), \quad P_8 = \frac{g_s}{16\pi^2} m_b (\bar{s}_L \sigma^{\mu\nu} T^a b_R) G_{\mu\nu}^a, \\ P_3 &= (\bar{s}_L \gamma_\mu b_L) \sum_q (\bar{q} \gamma^\mu q), \quad P_9 = \frac{e^2}{16\pi^2} (\bar{s}_L \gamma_\mu b_L) \sum_\ell (\bar{\ell} \gamma^\mu \ell), \\ P_4 &= (\bar{s}_L \gamma_\mu T^a b_L) \sum_q (\bar{q} \gamma^\mu T^a q), \quad P_{10} = \frac{e^2}{16\pi^2} (\bar{s}_L \gamma_\mu b_L) \sum_\ell (\bar{\ell} \gamma^\mu \gamma_5 \ell). \end{aligned} \quad (2.6)$$

In addition we have the following scalar-density operator with right-handed b -quark:³

$$P_0^\ell = \frac{e^2}{16\pi^2} (\bar{s}_L b_R) (\bar{\ell}_R \ell_L), \quad (2.7)$$

There is no reason to update the MFV analysis of precision $s \rightarrow d$ transitions of Ref. [15]. For completeness we state that for the rare decays $K \rightarrow \pi \nu \bar{\nu}$, we have the following simple effective hamiltonian,

$$\mathcal{H}_{\text{eff}}^{s \rightarrow d} = \frac{G_F \alpha_{\text{em}} (m_Z)}{\sqrt{2}} \sum_{\ell=e,\mu,\tau} \left(\frac{y_\nu}{2\pi \sin^2 \theta_W} P_{\nu\bar{\nu}} \right) + \text{h.c.}, \quad (2.8)$$

with the operator $P_{\nu\bar{\nu}}$ and the corresponding possible NP contribution $\delta C_{\nu\bar{\nu}}$,

$$P_{\nu\bar{\nu}} = (\bar{s} \gamma_\mu d) (\bar{\nu}_\ell \gamma^\mu (1 - \gamma_5) \nu_\ell), \quad y_\nu = \frac{1}{|V_{us}|} \left(\lambda_t (X_t + \delta C_{\nu\bar{\nu}}) + \text{Re} \lambda_c \tilde{P}_{u,c} \right), \quad (2.9)$$

and $\lambda_q = V_{qs}^* V_{qd}$, $X_t = 1.464 \pm 0.041$, $\tilde{P}_{u,c} = (0.2248)^4 P_{u,c}$ [35] and $P_{u,c} = 0.41 \pm 0.04$ [36–38].

We follow here the analysis of Ref. [15] and consider NP in the FCNC operators P_7, P_8, P_9, P_{10} and in the two scalar operators $P_{\nu\bar{\nu}}$ and P_0^ℓ only; as argued, in principle most of the possible NP contributions to the four-quark operators P_{1-6} could be reabsorbed into the Wilson coefficient of the FCNC operators. The NP contributions to the Wilson coefficients are parameterized as:

$$\delta C_i(\mu_b) = C_i^{\text{MFV}}(\mu_b) - C_i^{\text{SM}}(\mu_b). \quad (2.10)$$

where the $C_i^{\text{SM}}(\mu_b)$ are given in Table 1.

³ Within the MFV framework, the corresponding Wilson coefficient C_0^ℓ is related to $C_{Q_1} = m_b C_S$ and $C_{Q_2} = m_b C_P$ by $C_0^\ell = 2C_{Q_1} = -2C_{Q_2}$, where the operators are defined as $Q_1 = Q_S/m_b = \frac{e^2}{(16\pi^2)} (\bar{s}_L b_R) (\bar{\ell} \ell)$, $Q_2 = Q_P/m_b = \frac{e^2}{(16\pi^2)} (\bar{s}_L b_R) (\bar{\ell} \gamma_5 \ell)$.

$C_7^{\text{eff}}(\mu_b)$	$C_8^{\text{eff}}(\mu_b)$	$C_9(\mu_b)$	$C_{10}(\mu_b)$	$C_0^t(\mu_b)$
-0.2974	-0.1614	4.2297	-4.2068	0

Table 1: SM Wilson coefficients at $\mu_b = m_b^{\text{pole}}$ and $\mu_0 = 2M_W$ to NNLO accuracy in α_s .

3 Observables and theoretical uncertainties

We present the various $\Delta F = 1$ observables which we use in our MFV fit or which we want to constrain or predict. We focus on their dependence on the (non-standard) Wilson coefficients of the MFV effective theory and on the main sources of the theoretical uncertainty.

3.1 Radiative decay $\bar{B} \rightarrow X_{s,d}\gamma$

The branching fraction for $B \rightarrow X_q\gamma$ ($q = s, d$) for a photon energy cut $E_\gamma > E_0$ can be parameterized as

$$\text{BR}(B \rightarrow X_q\gamma)_{E_\gamma > E_0} = \text{BR}(B \rightarrow X_c e \bar{\nu})_{\text{exp}} \frac{6\alpha_{\text{em}}}{\pi C} \left| \frac{V_{tq}^* V_{tb}}{V_{cb}} \right|^2 \left[P(E_0) + N(E_0) \right], \quad (3.11)$$

where $\alpha_{\text{em}} = \alpha_{\text{em}}^{\text{on shell}}$ [39], $C = |V_{ub}|^2/|V_{cb}|^2 \times \Gamma[B \rightarrow X_c e \bar{\nu}]/\Gamma[B \rightarrow X_u e \bar{\nu}]$ and $P(E_0)$ and $N(E_0)$ denote the perturbative and nonperturbative contributions, respectively. The latter are normalized to the *charmless* semileptonic rate to separate the charm dependence. The perturbative part of the branching ratio of $\bar{B} \rightarrow X_s\gamma$ is known to NNLL precision [40], while the nonperturbative corrections are now estimated to be well below 10% [42]. The overall uncertainty consists of nonperturbative (5%), parametric (3%), perturbative (scale) (3%) and m_c -interpolation ambiguity (3%), which are added in quadrature. An additional scheme dependence in the determination of the pre-factor C has been found [41]; it is within the perturbative uncertainty of 3% [43]. The dependence of the dominating perturbative part from the Wilson coefficients can be parametrized [44] at NNL:

$$P(E_0) = P^{(0)}(\mu_b) + \left(\frac{\alpha_s(\mu_b)}{4\pi} \right) \left[P_1^{(1)}(\mu_b) + P_2^{(1)}(E_0, \mu_b) \right] + \mathcal{O}(\alpha_s^2(\mu_b)), \quad \text{where} \quad (3.12)$$

$$P^{(0)}(\mu_b) = \left[C_7^{(0)\text{eff}}(\mu_b) \right]^2, \quad P_1^{(1)}(\mu_b) = 2 C_7^{(0)\text{eff}}(\mu_b) C_7^{(1)\text{eff}}(\mu_b),$$

$$P_2^{(1)}(E_0, \mu_b) = \sum_{i,j=1}^8 C_i^{(0)\text{eff}}(\mu_b) C_j^{(0)\text{eff}}(\mu_b) K_{ij}^{(1)}(E_0, \mu_b). \quad (3.13)$$

The functions $K_{ij}^{(1)}$ can be found in Ref. [44]. The effective Wilson coefficients are given in the Appendix. We stress that we have used NNLL precision (means inclusion of $\mathcal{O}(\alpha_s^2(\mu_b))$ terms) in our numerical analysis.

The branching ratio of $\bar{B} \rightarrow X_d\gamma$ is only known to NLL QCD precision [45]. The error at this order is dominated by a large scale renormalization uncertainty of more than 12% and by uncertainties due to CKM matrix elements of 10%. However, in view of the large experimental error the NLL precision is still appropriate within our analysis.

3.2 Isospin asymmetry $\Delta_0(B \rightarrow K^* \gamma)$

Another important observable which is already measured is the isospin breaking ratio. It arises when the photon is emitted from the spectator quark:

$$\Delta_{0\pm} = \frac{\Gamma(\bar{B}^0 \rightarrow \bar{K}^{*0} \gamma) - \Gamma(B^\pm \rightarrow K^{*\pm} \gamma)}{\Gamma(\bar{B}^0 \rightarrow \bar{K}^{*0} \gamma) + \Gamma(B^\pm \rightarrow K^{*\pm} \gamma)}, \quad (3.14)$$

where the partial decay rates are CP -averaged. In the SM spectator-dependent effects enter only at the order Λ/m_b , whereas isospin-breaking in the form factors is expected to be a negligible effect. Therefore, the SM prediction is as small as $O(8\%)$. Moreover, a part of the Λ/m_b (leading) contribution cannot be calculated within the QCdf approach what leads to a large uncertainty [46]. However, the ratio is shown to be especially sensitive to NP effects in the penguin sector. The isospin asymmetry can be written as [46]:

$$\Delta_0 = \text{Re}(b_d - b_u), \quad (3.15)$$

where the spectator dependent coefficients b_q take the form: ⁴

$$b_q = \frac{12\pi^2 f_B Q_q}{\bar{m}_b T_1^{B \rightarrow K^*} a_7^c} \left(\frac{f_{K^*}^\perp}{\bar{m}_b} K_1 + \frac{f_{K^*} m_{K^*}}{6\lambda_B m_B} K_{2q} \right). \quad (3.16)$$

Here the coefficient a_7^c reads [48]:

$$a_7^c(K^* \gamma) = C_7(\mu_b) + \frac{\alpha_s(\mu_b) C_F}{4\pi} \left[C_2(\mu_b) G_2(x_{cb}) + C_8(\mu_b) G_8 \right] \\ + \frac{\alpha_s(\mu_h) C_F}{4\pi} \left[C_2(\mu_h) H_2(x_{cb}) + C_8(\mu_h) H_8 \right], \quad (3.17)$$

where $\mu_h = \sqrt{\Lambda_h \mu_b}$ is the spectator scale. The functions G_2, G_8, H_2 , and H_8 can be found in Ref. [48]. The functions K_1 and K_{2q} can be written in function of the Wilson coefficients C_i at scale μ_b [46]:

$$K_1 = - \left(C_6(\mu_b) + \frac{C_5(\mu_b)}{N} \right) F_\perp + \frac{C_F}{N} \frac{\alpha_s(\mu_b)}{4\pi} \left\{ \left(\frac{m_b}{m_B} \right)^2 C_8(\mu_b) X_\perp \right. \\ \left. - C_2(\mu_b) \left[\left(\frac{4}{3} \ln \frac{m_b}{\mu_b} + \frac{2}{3} \right) F_\perp - G_\perp(x_{cb}) \right] + r_1 \right\}, \quad (3.18)$$

$$K_{2q} = \frac{V_{us}^* V_{ub}}{V_{cs}^* V_{cb}} \left(C_2(\mu_b) + \frac{C_1(\mu_b)}{N} \right) \delta_{qu} + \left(C_4(\mu_b) + \frac{C_3(\mu_b)}{N} \right) \\ + \frac{C_F}{N} \frac{\alpha_s(\mu_b)}{4\pi} \left[C_2(\mu_b) \left(\frac{4}{3} \ln \frac{m_b}{\mu_b} + \frac{2}{3} - H_\perp(x_{cb}) \right) + r_2 \right], \quad (3.19)$$

where $x_{cb} = \frac{m_c^2}{m_b^2}$ and $N = 3$ and $C_F = 4/3$ are colour factors. The convolution integrals of the hard-scattering kernels with the meson distribution amplitudes $F_\perp, G_\perp, H_\perp$, and X_\perp can be found in Ref. [46], also the residual NLO corrections r_1 and r_2 .

⁴In this subsection we use the Wilson coefficients of the traditional basis [47].

Lattice QCD Group	Ref.	f_{B_s}	f_B
ETMC-11	[65]	232 ± 10 MeV	195 ± 12 MeV
Fermilab-MILC-11	[66, 67]	242 ± 9.5 MeV	197 ± 9 MeV
HPQCD-12	[68]	227 ± 10 MeV	191 ± 9 MeV
Average		234 ± 10 MeV	194 ± 10 MeV

Table 2: Average of lattice QCD results used in this work.

3.3 Leptonic decays $B_{s,d} \rightarrow \mu^+ \mu^-$

The rare decay $B_s \rightarrow \mu^+ \mu^-$ proceeds via Z^0 penguin and box diagrams in the SM. It is highly helicity-suppressed. However, for large values of $\tan \beta$ this decay can receive large contributions. In general, within MFV the pure leptonic decay $B_s \rightarrow \ell^+ \ell^-$ receive contributions only from the effective operators P_{10} and P_0^ℓ . These are free from the contamination of four-quark operators, which makes the generalization to the $b \rightarrow d$ case straightforward. The branching fraction in the MFV framework is given by

$$\text{BR}(B_s \rightarrow \mu^+ \mu^-) = \frac{G_F^2 \alpha^2}{64\pi^3} f_{B_s}^2 \tau_{B_s} m_{B_s}^3 |V_{tb} V_{ts}^*|^2 \sqrt{1 - \frac{4m_\mu^2}{m_{B_s}^2}} \quad (3.20)$$

$$\times \left[\left(1 - \frac{4m_\mu^2}{m_{B_s}^2}\right) \left| \left(\frac{m_{B_s}}{m_b + m_s}\right) (C_0^\mu/2) \right|^2 + \left| \left(\frac{m_{B_s}}{m_b + m_s}\right) (C_0^\mu/(-2)) + 2(C_{10}) \frac{m_\mu}{m_{B_s}} \right|^2 \right],$$

where f_{B_s} is the B_s decay constant, m_{B_s} is the B_s meson mass and τ_{B_s} is the B_s mean life.

The main theoretical uncertainty comes from the B_s decay constant f_{B_s} , which has recently been re-evaluated by independent lattice QCD groups of Table 2. Their 4.3% uncertainties agree, as do their results within these uncertainties, so that following Ref. [86] we have chosen an average of these three results in what follows. This implies a 8.7% uncertainty on the branching ratio. The most important parametric uncertainty comes from the CKM matrix element V_{ts} with 5%.

Within the MFV scenario the $B_d \rightarrow \ell^+ \ell^-$ rate can be obtained from the one of $B_s \rightarrow \ell^+ \ell^-$ with the exchange $(V_{ts}, m_{B_s}, m_s, f_{B_s}) \rightarrow (V_{td}, m_{B_d}, m_d, f_{B_d})$. This implies a very important MFV relation ($O(m_d/m_s)$ are neglected),

$$\frac{\Gamma(B_s \rightarrow \ell^+ \ell^-)}{\Gamma(B_d \rightarrow \ell^+ \ell^-)} \approx \frac{f_{B_s} m_{B_s}}{f_{B_d} m_{B_d}} \left| \frac{V_{ts}}{V_{td}} \right|^2. \quad (3.21)$$

3.4 Inclusive $\bar{B} \rightarrow X_s \mu^+ \mu^-$ and $\bar{B} \rightarrow X_s \tau^+ \tau^-$

The decay $B \rightarrow X_s \ell^+ \ell^-$ is particularly attractive because it offers several kinematic observables. The angular decomposition of the decay rate provides three independent observables, H_T , H_A and H_L , from which one can extract the short-distance electroweak Wilson coefficients that test for NP:

$$\frac{d^3\Gamma}{dq^2 dz} = \frac{3}{8} \left[(1 + z^2) H_T(q^2) + 2(1 - z^2) H_L(q^2) + 2z H_A(q^2) \right]. \quad (3.22)$$

Here $z = \cos \theta_\ell$, θ_ℓ is the angle between the negatively charged lepton and the \bar{B} meson in the center-of-mass frame of the dilepton system, and q^2 is the dilepton mass squared. H_A is equivalent to the forward-backward asymmetry, and the dilepton-mass spectrum is given by $H_T + H_L$. The observables mainly constrain the Wilson coefficients C_7^{eff} , C_9^{eff} and C_{10}^{eff} .

One defines perturbatively dominated (means theoretically clean) observables within two dilepton-mass windows avoiding the region with the $c\bar{c}$ resonances: the low- q^2 region ($1 \text{ GeV}^2 < q^2 < 6 \text{ GeV}^2$) and the high- q^2 region ($q^2 > 14.4 \text{ GeV}^2$).

In order to show the dependence of the observables on the Wilson coefficients, we use the conventions of Ref. [49]. We note that for the numerical evaluation we have used the conventions in Ref. [50], in particular we have chosen the charmless semileptonic decay rate as normalization. For the branching ratio within the MFV framework we find:

$$\begin{aligned}
\frac{d\text{BR}(B \rightarrow X_s \ell^+ \ell^-)}{d\hat{s}} &= \text{BR}(B \rightarrow X_c \ell \bar{\nu}) \frac{\alpha^2}{4\pi^2 f(z) \kappa(z)} \frac{|V_{tb} V_{ts}^*|^2}{|V_{cb}|^2} (1 - \hat{s})^2 \sqrt{1 - \frac{4\hat{m}_\ell^2}{\hat{s}}} \\
&\times \left\{ |C_9^{new}|^2 \left(1 + \frac{2\hat{m}_\ell^2}{\hat{s}}\right) (1 + 2\hat{s}) \left(1 + \frac{\alpha_s}{\pi} \tau_{99}(\hat{s})\right) + 4|C_7^{new}|^2 \left(1 + \frac{2\hat{m}_\ell^2}{\hat{s}}\right) \left(1 + \frac{2}{\hat{s}}\right) \left(1 + \frac{\alpha_s}{\pi} \tau_{77}(\hat{s})\right) \right. \\
&+ |C_{10}^{new}|^2 \left[(1 + 2\hat{s}) + \frac{2\hat{m}_\ell^2}{\hat{s}} (1 - 4\hat{s}) \right] \left(1 + \frac{\alpha_s}{\pi} \tau_{99}(\hat{s})\right) + 12\text{Re}(C_7^{new} C_9^{new*}) \left(1 + \frac{2\hat{m}_\ell^2}{\hat{s}}\right) \left(1 + \frac{\alpha_s}{\pi} \tau_{79}(\hat{s})\right) \\
&\left. + \frac{3}{4} |C_0^\ell|^2 (\hat{s} - 2\hat{m}_\ell^2) - 3\text{Re}(C_{10}^{new} C_0^{\ell*}) \hat{m}_\ell \right\} + \delta_{d\mathcal{B}/d\hat{s}}^{b\text{rems}} + \delta_{d\mathcal{B}/d\hat{s}}^{1/m_b^2} + \delta_{d\mathcal{B}/d\hat{s}}^{1/m_b^3} + \delta_{d\mathcal{B}/d\hat{s}}^{1/m_c^2} + \delta_{d\mathcal{B}/d\hat{s}}^{em}, \quad (3.23)
\end{aligned}$$

where the hat indicates a normalization by m_b . The functions τ_i correspond to specific bremsstrahlung terms. As indicated, further (but finite) bremsstrahlung, electromagnetic and power corrections have to be added, see Ref. [49] for more details. Our formula (3.23) is consistent with the results in Ref. [51].

For the dependence of the forward-backward asymmetry on the Wilson coefficients we find within the MFV setting:

$$\begin{aligned}
A_{FB}(\hat{s}) &= \int_0^1 dz \frac{d^2\text{BR}}{d\hat{s}dz} - \int_{-1}^0 dz \frac{d^2\text{BR}}{d\hat{s}dz} = -\text{B}(B \rightarrow X_c \ell \bar{\nu}) \frac{3\alpha^2}{4\pi^2 f(z) \kappa(z)} \frac{|V_{tb} V_{ts}^*|^2}{|V_{cb}|^2} (1 - \hat{s})^2 \left(1 - \frac{4\hat{m}_\ell^2}{\hat{s}}\right) \\
&\times \left\{ \text{Re}(C_9^{new} C_{10}^{new*}) \hat{s} \left(1 + \frac{\alpha_s}{\pi} \tau_{910}(\hat{s})\right) + 2\text{Re}(C_7^{new} C_{10}^{new*}) \left(1 + \frac{\alpha_s}{\pi} \tau_{710}(\hat{s})\right) \right. \\
&\left. + \text{Re}\left((C_9^{new}/2 + C_7^{new}) C_0^{\ell*}\right) \hat{m}_\ell \right\} + \delta_{A_{FB}}^{1/m_b^2}(\hat{s}) + \delta_{A_{FB}}^{1/m_c^2}(\hat{s}) + \delta_{A_{FB}}^{b\text{rems}}(\hat{s}) + \delta_{A_{FB}}^{em}(\hat{s}). \quad (3.24)
\end{aligned}$$

We note that Eq. (3.24) is consistent with the results in Ref. [51], but disagrees with Refs. [52, 53] for the scalar contributions. The *new* Wilson coefficients are defined in Ref. [49] and are given in the Appendix.

In the low- q^2 region the theoretical uncertainty is around 7% for the branching ratio, however there is an additional 5% uncertainty due to nonlocal power corrections to be added [50]. In the high- q^2 region, one encounters the breakdown of the heavy-mass expansion at the endpoint. However, for an integrated high- q^2 spectrum an effective expansion exists in inverse powers of $m_b^{\text{eff}} = m_b \times (1 - \sqrt{s_{\text{min}}})$ rather than m_b . The resulting large theoretical uncertainties in the high- q^2 due to the power corrections of around 25% could be significantly reduced by normalizing the $\bar{B} \rightarrow X_s \ell^+ \ell^-$ decay rate to the semileptonic $\bar{B} \rightarrow X_u \ell \bar{\nu}$ decay rate with the same q^2 cut [54]. For example, the uncertainty due to the dominating $1/m_b^3$ term would be reduced from 19% to 9% [50].

3.5 Exclusive decay $B \rightarrow K^* \ell \ell$

The exclusive semi-leptonic penguin modes offer a larger variety of experimentally accessible observables than do the inclusive ones, but the hadronic uncertainties in the theoretical predictions are in general larger.

The physics opportunities of $B \rightarrow K^* \ell \ell$ ($\ell = e, \mu, \tau$) decays depend strongly on the measurement of their angular distributions. This decay with K^* on the mass shell has a 4-fold differential distribution [57, 58]

$$\frac{d^4\Gamma[B \rightarrow K^*(\rightarrow K\pi)\ell\ell]}{dq^2 d\cos\theta_l d\cos\theta_K d\phi} = \frac{9}{32\pi} \sum_i J_i(q^2) g_i(\theta_l, \theta_K, \phi), \quad (3.25)$$

w.r.t. the dilepton invariant mass q^2 and the angles θ_l , θ_K , and ϕ (as defined in [55]). It offers 12 observables $J_i(q^2)$, from which all other known ones can be derived upon integration over appropriate combinations of angles.

The J_i depend on products of the eight theoretical complex K^* spin amplitudes A_i , $A_{\perp,\parallel,0}^{L,R}$, A_t , A_s . The J_i are bi-linear functions of the spin amplitudes such as

$$J_s^1 = \frac{3}{4} \left[|A_{\perp}^L|^2 + |A_{\parallel}^L|^2 + |A_{\perp}^R|^2 + |A_{\parallel}^R|^2 \right], \quad (3.26)$$

with the expression for the eleven other J_i terms given for example in [56, 58, 59].

The dilepton invariant mass spectrum for $B \rightarrow K^* \ell^+ \ell^-$ can be recovered after integrating the 4-differential distribution over all angles, while the (normalized) forward-backward asymmetry A_{FB} can be defined after full ϕ and θ_{K^*} integration [60] ($J_i \equiv 2J_i^s + J_i^c$):

$$\frac{d\Gamma}{dq^2} = \frac{3}{4} \left(J_1 - \frac{J_2}{3} \right), \quad A_{\text{FB}}(q^2) \equiv \left[\int_{-1}^0 - \int_0^1 \right] d\cos\theta_l \frac{d^2\Gamma}{dq^2 d\cos\theta_l} \Big/ \frac{d\Gamma}{dq^2} = -\frac{3}{8} \frac{J_6}{d\Gamma/dq^2}. \quad (3.27)$$

Moreover, the fraction of the longitudinal polarized K^* is given by $F_L = (3J_1^c - J_2^c)/(4d\Gamma/dq^2)$. These three observables represent the *early* ones, which have been measured already by the B factories and now with much better precision by the LHCb experiment.

With more luminosity, theoretically much cleaner angular observables will be available. In the low- and high- q^2 region it is always appropriate to design optimized observables by using specifically chosen normalizations for the independent set of observables. In the low- q^2 region, specific ratios of observables allow for a complete cancellation of the hadronic uncertainties due to the form factors in leading order and, thus, for a high increase in the sensitivity to new physics structures [55, 59], for example the transversity amplitudes:

$$A_T^{(2)} = \frac{1}{2} \frac{J_3}{J_2^s}, \quad A_T^{(3)} = \sqrt{\frac{4J_4^2 + \beta_l^2 J_7^2}{-2J_2^c(2J_2^s + J_3)}}, \quad A_T^{(4)} = \sqrt{\frac{\beta_l^2 J_5^2 + 4J_8^2}{4J_4^2 + \beta_l^2 J_7^2}}. \quad (3.28)$$

In the high- q^2 region, two groups of ratios of observables can be constructed which dominantly depend either on short- or on long-distance physics [61, 62]. In addition to the $A_T^{(i)}$ observables some new transversity observables were proposed:

$$H_T^{(1)} = \frac{\sqrt{2}J_4}{\sqrt{-J_2^c(2J_2^s - J_3)}}, \quad H_T^{(2)} = \frac{\beta_l J_5}{\sqrt{-2J_2^c(2J_2^s + J_3)}}, \quad H_T^{(3)} = \frac{\beta_l J_6}{2\sqrt{(2J_2^s)^2 - J_3^2}}. \quad (3.29)$$

In the high- q^2 region $H_T^{(2,3)}$ depend only on short-distance information in leading order, while F_L and $A_T^{(2,3)}$ depend only on long-distance quantities.⁵

The theoretical treatment in the low- and high- q^2 is based on different theoretical concepts. Thus, the consistency of the consequences out of the two sets of measurements will allow for an important crosscheck.

In the low- q^2 region, the up-to-date description of exclusive heavy-to-light $B \rightarrow K^* \ell^+ \ell^-$ decays is the method of QCD-improved Factorization (QCDF) and its field-theoretical formulation of Soft-Collinear Effective Theory (SCET). In the combined limit of a heavy b -quark and of an energetic K^* meson, the decay amplitude factorizes to leading order in Λ/m_b and to all orders in α_s into process-independent non-perturbative quantities like $B \rightarrow K^*$ form factors and light-cone distribution amplitudes (LCDAs) of the heavy (light) mesons and perturbatively calculable quantities, which are known to $O(\alpha_s^1)$ [16, 17]. Further, the *seven* a priori independent $B \rightarrow K^*$ QCD form factors reduce to *two* universal *soft* form factors $\xi_{\perp, \parallel}$ [64]. The factorization formula applies well in the range of the dilepton mass range, $1 \text{ GeV}^2 < q^2 < 6 \text{ GeV}^2$.

Taking into account all these simplifications the various K^* spin amplitudes at leading order in Λ_{QCD}/m_b and α_s turn out to be linear in the soft form factors $\xi_{\perp, \parallel}$ and also in the short-distance Wilson coefficients which allows to design a set of optimized observables in which any soft form factor dependence (and its corresponding uncertainty) cancels out for all low dilepton masses q^2 at leading order in α_s and Λ_{QCD}/m_b [55, 59]:

$$A_{\perp}^{L,R} = \sqrt{2} N m_B (1 - \hat{s}) \left[(\mathcal{C}_9^{\text{eff}} \mp \mathcal{C}_{10}) + \frac{2\hat{m}_b}{\hat{s}} \mathcal{C}_7^{\text{eff}} \right] \xi_{\perp}(E_{K^*}), \quad (3.30a)$$

$$A_{\parallel}^{L,R} = -\sqrt{2} N m_B (1 - \hat{s}) \left[(\mathcal{C}_9^{\text{eff}} \mp \mathcal{C}_{10}) + \frac{2\hat{m}_b}{\hat{s}} \mathcal{C}_7^{\text{eff}} \right] \xi_{\perp}(E_{K^*}), \quad (3.30b)$$

$$A_0^{L,R} = -\frac{N m_B}{2\hat{m}_{K^*} \sqrt{\hat{s}}} (1 - \hat{s})^2 \left[(\mathcal{C}_9^{\text{eff}} \mp \mathcal{C}_{10}) + 2\hat{m}_b \mathcal{C}_7^{\text{eff}} \right] \xi_{\parallel}(E_{K^*}), \quad (3.30c)$$

$$A_t = \frac{N m_B}{\hat{m}_{K^*} \sqrt{\hat{s}}} (1 - \hat{s})^2 \left[\mathcal{C}_{10} - \frac{q^2}{4m_{\ell} m_b} C_0^{\ell} \right] \xi_{\parallel}(E_{K^*}), \quad (3.30d)$$

$$A_S = \frac{N m_B^2}{2\hat{m}_{K^*} m_b} (1 - \hat{s})^2 \left[(-1) C_0^{\ell} \right] \xi_{\parallel}(E_{K^*}), \quad (3.30e)$$

with $\hat{s} = q^2/m_B^2$, $\hat{m}_i = m_i/m_B$. Here we neglect terms of $O(\hat{m}_{K^*}^2)$ but we include these terms in our numerical analysis. The factor N collects all pre-factors and can be found in Ref. [55, 59]. The soft form factors are fixed in a specific factorization scheme using QCD sum rule techniques as discussed in the Appendix.

However, in the early observables, namely $d\Gamma/dq^2$, A_{FB} , F_L there is still a large theoretical uncertainty due to the form factors which do not cancel out to first order in these cases.

Within the QCDF/SCET approach, a general, quantitative method to estimate the important Λ_{QCD}/m_b corrections to the heavy quark limit is missing. In semileptonic decays a simple dimensional estimate of 10% is often used. Under the assumption that the main part of the Λ_{QCD}/m_b corrections is included in the full form factors, the difference of the theoretical results using the full QCD form

⁵There are three observables which are already measured beyond the early observables mentioned above: $S_3 = (J_3 + \bar{J}_3)/[d(\Gamma + \bar{\Gamma})/dq^2]$, A_{im} , and the isospin asymmetry, but all three observables have no significant impact on the MFV scenario yet.

factors on one hand and the soft form factors on the other hand confirms this simple dimensional estimate. In fact, the comparison of the approaches leads to a 7% shift of the central value.

The low-hadronic recoil region is characterized by large values of the dilepton invariant mass $q^2 \gtrsim (14 - 15) \text{ GeV}^2$ above the two narrow resonances of J/ψ and $\psi(2S)$. It is shown that local operator product expansion is applicable ($q^2 \sim m_b^2$) [18, 19] and it allows to obtain the $B \rightarrow K^* \ell^+ \ell^-$ matrix element in a systematic expansion in α_s and in Λ/m_b . Most important, the leading power corrections are shown to be suppressed by $(\Lambda_{\text{QCD}}/m_b)^2$ or $\alpha_s \Lambda_{\text{QCD}}/m_b$ [19] and to contribute only at the few percent level. The only caveat is that heavy-to-light form factors are known only from extrapolations from LCSR calculations at low- q^2 at present. But this may improve in the future when direct lattice calculations in the high- q^2 are available [61].

There are improved Isgur-Wise relations between the form factors in leading power of Λ/m_b . Their application and the introduction of specific modified Wilson coefficients lead to simple expressions for the K^* spin amplitudes to leading order in $1/m_b$ in the low recoil region, for example we have [61]

$$A_{\perp}^{L,R} = +i \left\{ (C_9^{\text{eff,mod}} \mp C_{10}) + \kappa \frac{2\hat{m}_b}{\hat{s}} C_7^{\text{eff,mod}} \right\} f_{\perp}, \quad (3.31)$$

$$A_{\parallel}^{L,R} = -i \left\{ (C_9^{\text{eff,mod}} \mp C_{10}) + \kappa \frac{2\hat{m}_b}{\hat{s}} C_7^{\text{eff,mod}} \right\} f_{\parallel}, \quad (3.32)$$

$$A_0^{L,R} = -i \left\{ (C_9^{\text{eff,mod}} \mp C_{10}) + \kappa \frac{2\hat{m}_b}{\hat{s}} C_7^{\text{eff,mod}} \right\} f_0, \quad (3.33)$$

where the form factors f_{\perp} , f_{\parallel} , and f_0 are linearly connected to the QCD form factors (see Ref. [61]). The *modified* effective Wilson coefficients introduced in Ref. [18] are given in the Appendix. Then, the three considered observables at leading order can be written in the high- q^2 region as [61]

$$\frac{d\Gamma}{dq^2} = 2\rho_1 \times (f_0^2 + f_{\perp}^2 + f_{\parallel}^2), \quad A_{\text{FB}} = 3 \frac{\rho_2}{\rho_1} \times \frac{f_{\perp} f_{\parallel}}{(f_0^2 + f_{\perp}^2 + f_{\parallel}^2)}, \quad F_{\text{L}} = \frac{f_0^2}{f_0^2 + f_{\perp}^2 + f_{\parallel}^2}, \quad (3.34)$$

where only the two independent combinations of Wilson coefficients enter, namely

$$\rho_1 \equiv \left| C_9^{\text{eff}} + \kappa \frac{2\hat{m}_b}{\hat{s}} C_7^{\text{eff}} \right|^2 + |C_{10}|^2, \quad \rho_2 \equiv \text{Re} \left\{ \left(C_9^{\text{eff}} + \kappa \frac{2\hat{m}_b}{\hat{s}} C_7^{\text{eff}} \right) C_{10}^* \right\}. \quad (3.35)$$

ρ_1 and ρ_2 are shown to be largely μ -scale independent [18].

As mentioned above, the leading power corrections of the OPE arise at $\mathcal{O}(\alpha_s \Lambda/m_b, m_c^4/Q^4)$ and of the order of a few percent. The Λ/m_b corrections to the amplitudes from the form factor relations are parametrically suppressed as well, by small dipole coefficients, such that one can estimate the leading power correction from the form factor relations to the decay amplitudes as order $(2C_7^{\text{eff}}/C_9^{\text{eff}})\Lambda/m_b$. So in general, the dominant power corrections to the transversity amplitudes are of the order of a few percent [61].

4 Numerical details

Within our numerical analysis we use the most recent LHCb results for the exclusive decays $B_s \rightarrow \mu^+ \mu^-$ and $B \rightarrow K^* \mu^+ \mu^-$, and Belle, Babar and CDF results for the other decays. The experimental values are provided in Table 3. For comparison, we also consider the pre-LHCb data as given in Table 4.

Observable	Experiment	SM prediction
$\text{BR}(B \rightarrow X_s \gamma)$	$(3.55 \pm 0.24 \pm 0.09) \times 10^{-4}$ [77]	$(3.08 \pm 0.24) \times 10^{-4}$
$\Delta_0(B \rightarrow K^* \gamma)$	$(5.2 \pm 2.6 \pm 0.09) \times 10^{-2}$ [77]	$(8.0 \pm 3.9) \times 10^{-2}$
$\text{BR}(B \rightarrow X_d \gamma)$	$(1.41 \pm 0.57) \times 10^{-5}$ [78, 79]	$(1.49 \pm 0.30) \times 10^{-5}$
$\text{BR}(B_s \rightarrow \mu^+ \mu^-)$	$< 4.5 \times 10^{-9}$ [80]	$(3.53 \pm 0.38) \times 10^{-9}$
$\langle d\text{BR}/dq^2(B \rightarrow K^* \mu^+ \mu^-) \rangle_{q^2 \in [1,6] \text{GeV}^2}$	$(0.42 \pm 0.04 \pm 0.04) \times 10^{-7}$ [81]	$(0.47 \pm 0.27) \times 10^{-7}$
$\langle d\text{BR}/dq^2(B \rightarrow K^* \mu^+ \mu^-) \rangle_{q^2 \in [14.18, 16] \text{GeV}^2}$	$(0.59 \pm 0.07 \pm 0.04) \times 10^{-7}$ [81]	$(0.71 \pm 0.18) \times 10^{-7}$
$\langle A_{FB}(B \rightarrow K^* \mu^+ \mu^-) \rangle_{q^2 \in [1,6] \text{GeV}^2}$	$-0.18 \pm 0.06 \pm 0.02$ [81]	-0.06 ± 0.05
$\langle A_{FB}(B \rightarrow K^* \mu^+ \mu^-) \rangle_{q^2 \in [14.18, 16] \text{GeV}^2}$	$0.49 \pm 0.06 \pm 0.05$ [81]	0.44 ± 0.10
$q_0^2(A_{FB}(B \rightarrow K^* \mu^+ \mu^-))$	$4.9_{-1.3}^{+1.1} \text{GeV}^2$ [81]	$4.26 \pm 0.34 \text{GeV}^2$
$\langle F_L(B \rightarrow K^* \mu^+ \mu^-) \rangle_{q^2 \in [1,6] \text{GeV}^2}$	$0.66 \pm 0.06 \pm 0.04$ [81]	0.72 ± 0.13
$\text{BR}(B \rightarrow X_s \mu^+ \mu^-)_{q^2 \in [1,6] \text{GeV}^2}$	$(1.60 \pm 0.68) \times 10^{-6}$ [82, 83]	$(1.78 \pm 0.16) \times 10^{-6}$
$\text{BR}(B \rightarrow X_s \mu^+ \mu^-)_{q^2 > 14.4 \text{GeV}^2}$	$(4.18 \pm 1.35) \times 10^{-7}$ [82, 83]	$(2.19 \pm 0.44) \times 10^{-7}$

Table 3: Input observables: The experimental data represent the most recent one. The updated SM predictions are based on the input parameters given in Table 5.

There is a remark in order regarding the branching fraction of $B_s \rightarrow \mu^+ \mu^-$. Its value provided by the experiments corresponds to an untagged value, while the theoretical predictions are CP-averaged. As pointed out recently in [87, 88], the untagged branching ratio is related to the CP-averaged one by:

$$\text{BR}^{\text{untag}}(B_s \rightarrow \mu^+ \mu^-) = \left[\frac{1 + \mathcal{A}_{\Delta\Gamma} y_s}{1 - y_s^2} \right] \text{BR}(B_s \rightarrow \mu^+ \mu^-), \quad (4.36)$$

where

$$y_s \equiv \frac{1}{2} \tau_{B_s} \Delta\Gamma_s = 0.088 \pm 0.014, \quad (4.37)$$

and

$$\mathcal{A}_{\Delta\Gamma} = \frac{|P|^2 \cos(2\varphi_P) - |S|^2 \cos(2\varphi_S)}{|P|^2 + |S|^2}, \quad (4.38)$$

with

$$S \equiv \sqrt{1 - 4 \frac{m_\mu^2}{M_{B_s}^2} \frac{M_{B_s}^2}{2m_\mu} \frac{1}{m_b + m_s} \frac{C_0^\ell/2}{C_{10}^{SM}}}, \quad (4.39)$$

$$P \equiv \frac{C_{10}}{C_{10}^{SM}} + \frac{M_{B_s}^2}{2m_\mu} \frac{1}{m_b + m_s} \frac{-C_0^\ell/2}{C_{10}^{SM}}, \quad (4.40)$$

and

$$\varphi_S = \arg(S), \quad \varphi_P = \arg(P). \quad (4.41)$$

The obtained branching ratio can then be directly compared to the experimental result.

The SM predictions entering the MFV-fit are based on the theoretical analyses given in Section 3. We have used the input parameters of Table 5 and the program `SuperIso v3.3` [75, 76] in order to update SM predictions. They are given in Table 3.

To obtain constraints on the Wilson coefficients, we scan over δC_7 , δC_8 , δC_9 , δC_{10} and δC_0^ℓ . For each point, we then compute the flavour observables using `SuperIso v3.3` [75, 76] and compare with the experimental results by calculating χ^2 as:

$$\chi^2 = \sum_i \frac{(O_i^{\text{exp}} - O_i^{\text{th}})^2}{(\sigma_i^{\text{exp}})^2 + (\sigma_i^{\text{th}})^2}, \quad (4.42)$$

Observable	Experiment
$\text{BR}(B \rightarrow X_s \gamma)$	$(3.55 \pm 0.24 \pm 0.09) \times 10^{-4}$ [77]
$\Delta_0(B \rightarrow K^* \gamma)$	$(5.2 \pm 2.6 \pm 0.09) \times 10^{-2}$ [77]
$\text{BR}(B \rightarrow X_d \gamma)$	$(1.41 \pm 0.57) \times 10^{-5}$ [78, 79]
$\text{BR}(B_s \rightarrow \mu^+ \mu^-)$	$< 5.8 \times 10^{-8}$ [84]
$\langle d\text{BR}/dq^2(B \rightarrow K^* \ell^+ \ell^-) \rangle_{q^2 \in [1,6] \text{GeV}^2}$	$(0.32 \pm 0.11 \pm 0.03) \times 10^{-7}$ [85]
$\langle d\text{BR}/dq^2(B \rightarrow K^* \mu^+ \mu^-) \rangle_{q^2 \in [14.18, 16] \text{GeV}^2}$	$(0.83 \pm 0.20 \pm 0.07) \times 10^{-7}$ [85]
$\langle A_{FB}(B \rightarrow K^* \mu^+ \mu^-) \rangle_{q^2 \in [1,6] \text{GeV}^2}$	$0.43 \pm 0.36 \pm 0.06$ [85]
$\langle A_{FB}(B \rightarrow K^* \mu^+ \mu^-) \rangle_{q^2 \in [14.18, 16] \text{GeV}^2}$	$0.42 \pm 0.16 \pm 0.09$ [85]
$\langle F_L(B \rightarrow K^* \mu^+ \mu^-) \rangle_{q^2 \in [1,6] \text{GeV}^2}$	$0.50 \pm 0.30 \pm 0.03$ [85]
$\text{BR}(B \rightarrow X_s \mu^+ \mu^-)_{q^2 \in [1,6] \text{GeV}^2}$	$(1.60 \pm 0.68) \times 10^{-6}$ [82, 83]
$\text{BR}(B \rightarrow X_s \mu^+ \mu^-)_{q^2 > 14.4 \text{GeV}^2}$	$(4.18 \pm 1.35) \times 10^{-7}$ [82, 83]

Table 4: Experimental data used for pre-LHCb fit.

$m_B = 5.27950 \text{ GeV}$	[71]	$m_{B_s} = 5.3663 \text{ GeV}$	[71]
$m_{K^*} = 0.89594 \text{ GeV}$	[71]	$ V_{tb} V_{ts}^* = 0.0403^{+0.0011}_{-0.0007}$	[71]
$m_b^{MS}(m_b) = 4.19^{+0.18}_{-0.06} \text{ GeV}$	[71]	$m_c^{MS}(m_c) = 1.29^{+0.05}_{-0.11} \text{ GeV}$	[71]
$m_t^{pole} = 172.9 \pm 0.6 \pm 0.9 \text{ GeV}$	[71]	$m_\mu = 0.105658 \text{ GeV}$	[71]
$\alpha_s(M_Z) = 0.1184 \pm 0.0007$	[71]	$\hat{\alpha}_{em}(M_Z) = 1/127.916$	[71]
$\alpha_s(\mu_b) = 0.2161$		$\hat{\alpha}_{em}(m_b) = 1/133$	
$\sin^2 \hat{\theta}_W(M_Z) = 0.23116(13)$	[71]	$G_F/(\hbar c)^3 = 1.16637(1) \text{ GeV}^{-2}$	[71]
$f_B = 194 \pm 10 \text{ MeV}$	Table 2	$\tau_B = 1.519 \pm 0.007 \text{ ps}$	[71]
$f_{B_s} = 234 \pm 10 \text{ MeV}$	Table 2	$\tau_{B_s} = 1.472 \pm 0.026 \text{ ps}$	[71]
$f_{K^*, \perp}(1 \text{ GeV}) = 0.185 \pm 0.009 \text{ GeV}$	[72]	$f_{K^*, \parallel} = 0.220 \pm 0.005 \text{ GeV}$	[72]
$a_{1, \perp}(1 \text{ GeV}) = 0.10 \pm 0.07$	[73]	$a_{1, \parallel}(1 \text{ GeV}) = 0.10 \pm 0.07$	[73]
$a_{2, \perp}(1 \text{ GeV}) = 0.13 \pm 0.08$	[73]	$a_{2, \parallel}(1 \text{ GeV}) = 0.09 \pm 0.05$	[73]
$\lambda_{B, +}(1 \text{ GeV}) = 0.46 \pm 0.11 \text{ GeV}$	[74]		
$\mu_b = m_b^{pole}$		$\mu_0 = 2M_W$	
$\mu_f = \sqrt{0.5} \times \mu_b \text{ GeV}$	[17]		

Table 5: Input parameters.

where O_i^{exp} and O_i^{th} are the central values of the experimental result and theoretical prediction of observable i respectively, and σ_i^{exp} and σ_i^{th} are the experimental and theoretical errors respectively. The global fits are obtained by minimization of the χ^2 . For LHCb fits, we consider the measurements of the observables given in Table 3 while for the pre-LHCb the measurements of Table 4 are considered.

5 Results

5.1 Separate bounds

We first study the individual constraints from the observables described in Section 3. The main players in our analysis are the radiative decay $\bar{B} \rightarrow X_s \gamma$, the leptonic decay $B \rightarrow \mu^+ \mu^-$, and the semileptonic decays $\bar{B} \rightarrow X_s/K^* \mu^- \mu^-$.

Figure 1 shows that similar zones are probed by the inclusive decays $\bar{B} \rightarrow X_s \gamma$ and $\bar{B} \rightarrow X_d \gamma$. The bounds in the $(\delta C_7, \delta C_8)$ planes induced by the two inclusive decays are nicely consistent with each other as expected in the MFV framework which predicts a strong correlation between the two decays. Clearly, due to the smaller theoretical and experimental error the $\bar{B} \rightarrow X_s \gamma$ bound is much stronger.

In the previous MFV analysis [15] the approximation was used that the NP contributions to the electromagnetic and chromomagnetic operators appear in a fixed linear combination, namely $\delta C_7 + 0.3\delta C_8$. This additional assumption was necessary in the previous analysis due to the limited number of independent experimental measurements. The correlations between δC_7 and δC_8 , shown in Figure 1, do not support this simplifying assumption.

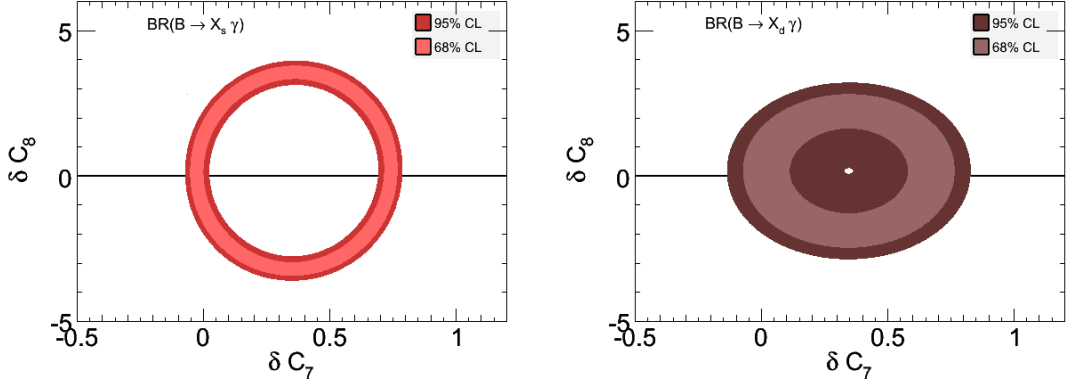


Figure 1: 68% and 95% CL bounds on δC_7 and δC_8 induced by the inclusive decays $\bar{B} \rightarrow X_s \gamma$ (left) and $\bar{B} \rightarrow X_d \gamma$ (right).

The isospin asymmetry in the exclusive mode $B \rightarrow K^* \gamma$ brings complementary information to the inclusive branching ratios. Figure 2 shows that the isospin asymmetry seems to favor opposite signs for δC_7 and δC_8 .

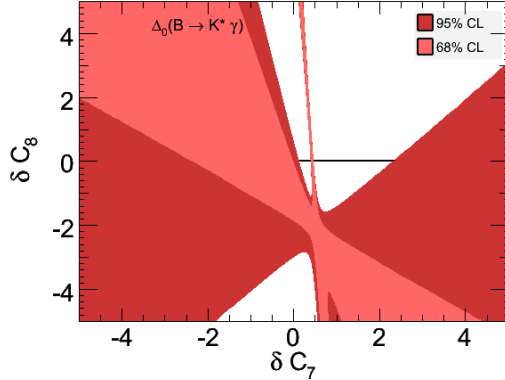


Figure 2: 68% and 95% bounds on δC_7 and δC_8 induced by the isospin asymmetry in $B \rightarrow K^* \gamma$.

The leptonic decays $B_s \rightarrow \mu^+ \mu^-$ and $B_d \rightarrow \mu^+ \mu^-$ are sensitive for δC_{10} and the scalar contribution δC_0^ℓ . The shapes in the corresponding correlation plots induced by the two leptonic decays are very similar, thus, highly consistent with each other as can be seen in Figure 3. This feature strongly supports the MFV hypothesis which predicts a strong correlation between these two decays as given in Eq. (3.21). Of course, the experimental limit for the decay $B_s \rightarrow \mu^+ \mu^-$ is much tighter and therefore the present constraints are much stronger. We therefore take the decay $B_d \rightarrow \mu^+ \mu^-$ out of the global MFV fit and will make a prediction for this decay within the MFV framework below.

We notice that the constraint on the scalar coefficient induced by the decay $B_s \rightarrow \mu^+ \mu^-$ is very strong and a large scalar contribution is not allowed anymore.

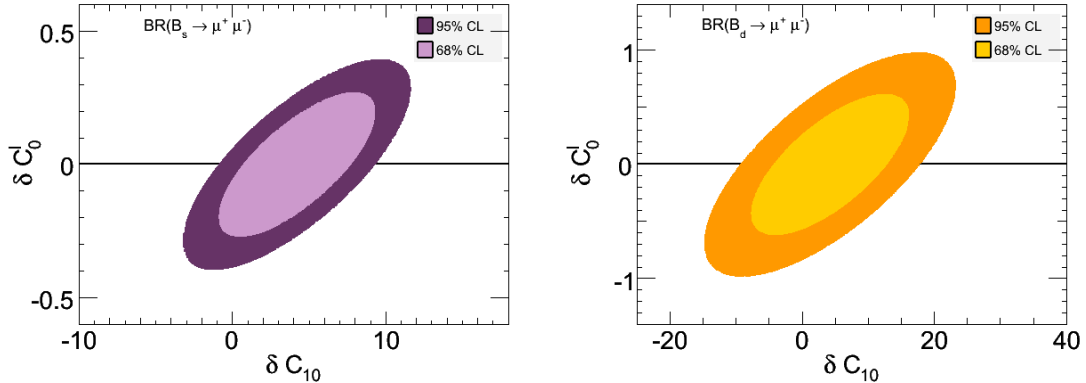


Figure 3: 68% and 95% CL bounds on δC_{10} and δC_0^l induced by the decays $B_s \rightarrow \mu^+ \mu^-$ (left), $B_d \rightarrow \mu^+ \mu^-$ (right).

The low- q^2 data of the inclusive decay $\bar{B} \rightarrow X_s \mu^+ \mu^-$ and of the exclusive decay $B \rightarrow K^* \mu^+ \mu^-$ have similar constraining power, as can be seen in Figure 4. It is nontrivial that the correlation plots of the various δC_i look almost identical for the inclusive and the exclusive mode. $\bar{B} \rightarrow X_s \mu^+ \mu^-$ has small theoretical errors and large experimental errors, while the situation is reversed for $B \rightarrow K^* \mu^+ \mu^-$. A statistical combination of both allows to enhance their effect. However, one realizes the potential of the inclusive mode if one takes into account the fact that the recent Babar and Belle measurements of the inclusive branching ratios [82, 83] only use less than a quarter of the available data sets of the B factories. The constraints on C_{10} are similar to those from $B_s \rightarrow \mu^+ \mu^-$, but contrary to $B_s \rightarrow \mu^+ \mu^-$, the constraints on the scalar contributions here is very weak.

Finally, we note that the allowed values of δC_9 and δC_{10} are much smaller in specific NP models than within a model-independent analysis, so for example the structure of the CMSSM already bounds their values significantly before any experimental data is used (see Ref. [86]).

5.2 Fit results

We made two global MFV fits in order to make the significance of the latest LHCb data manifest, see Figure 5. First we have used the experimental data before the start of the LHCb experiment (pre-LHCb, right plots). These measurements are listed in Table 4. Then we have included the latest LHCb measurements given in Table 3 (post-LHCb, left plots).

Here C_8 is mostly constrained by $\bar{B} \rightarrow X_{s,d} \gamma$, while C_7 is constrained by many other observables as well. C_9 is highly constrained by $b \rightarrow s \mu^+ \mu^-$ (inclusive and exclusive). C_{10} is in addition further constrained by $B_s \rightarrow \mu^+ \mu^-$. C_0^l is dominantly constrained by $B_s \rightarrow \mu^+ \mu^-$.

There are always two allowed regions at 95% CL in the correlation plots within the post-LHCb fit; one corresponds to SM-like MFV coefficients and one to coefficients with flipped sign. The allowed region with the SM is more favored. The various δC_i -correlation plots show the flipped-sign for C_7 is only possible if C_9 and C_{10} receive large non-standard contributions which finally also change the sign of these coefficients.

We have also studied the impact of the LHCb measurements of the branching ratio, of the forward-backward asymmetry, and of the K^* polarization within the exclusive decay $B \rightarrow K^* \ell^+ \ell^-$ by taking these LHCb measurements out of the fit. The results in Table 6 show that these pieces of experimental information from the LHCb experiment are very important. They significantly reduce the allowed areas for δC_9 and δC_{10} .

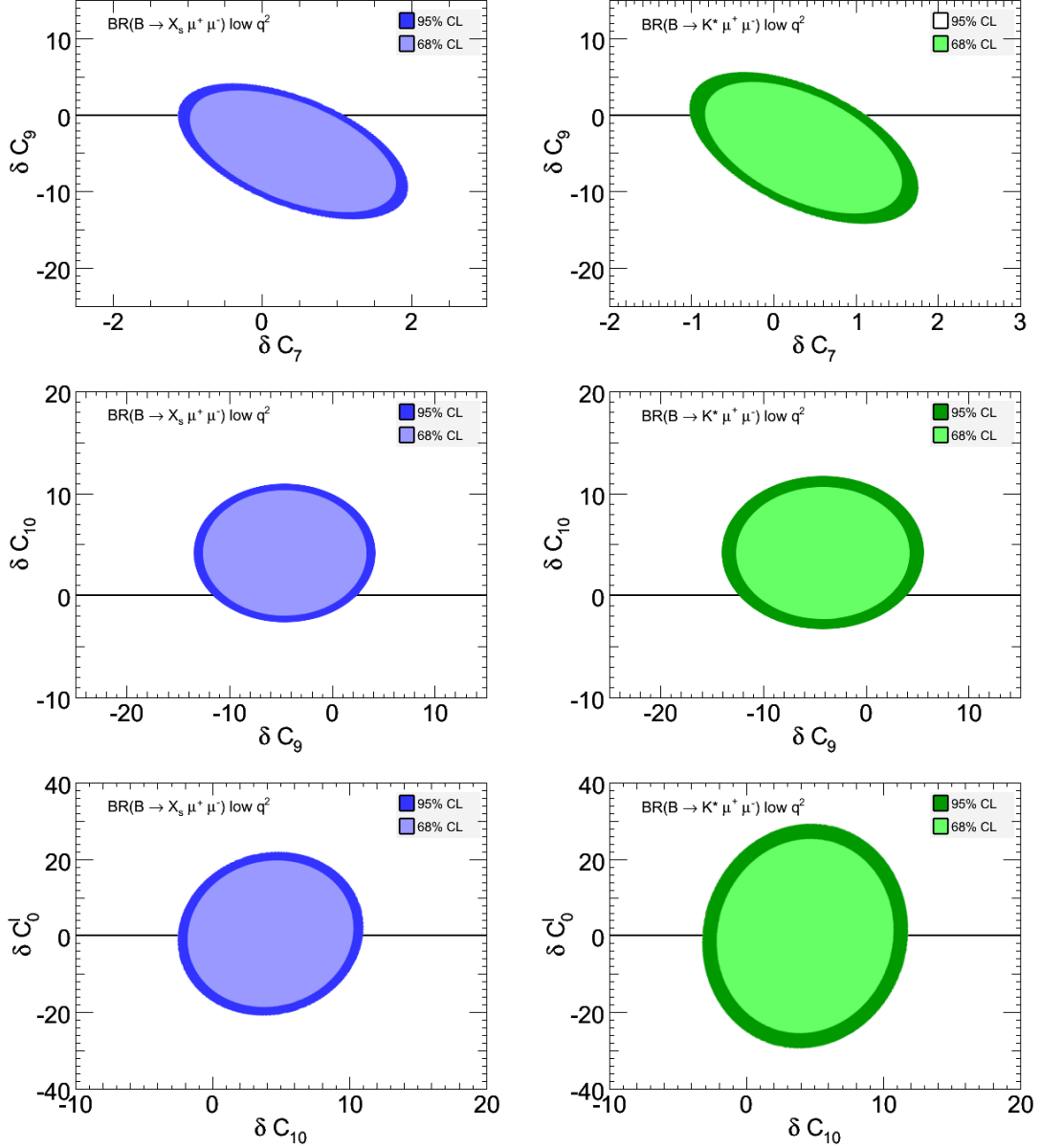


Figure 4: 68% and 95% CL bounds on various δC_i induced by the decays $B \rightarrow X_s \mu^+ \mu^-$ (left) and $B \rightarrow K^* \mu^+ \mu^-$ (right) at low- q^2 .

5.3 Predictions within the MFV benchmark

With the help of the results of the global fit, which restricts the NP contributions δC_i , we can now derive several interesting predictions of observables which are not yet well measured. This analysis allows to spot these observables which still allow for relatively large deviations from the SM even in the MFV benchmark scenario.

- For the branching ratio of the decay $\bar{B} \rightarrow X_s \tau \tau$ we get the 95%CL bounds

$$0.2 \times 10^{-7} < \text{BR}(\bar{B} \rightarrow X_s \tau^+ \tau^-)_{q^2 > 14.4 \text{ GeV}^2} < 3.7 \times 10^{-7}. \quad (5.43)$$

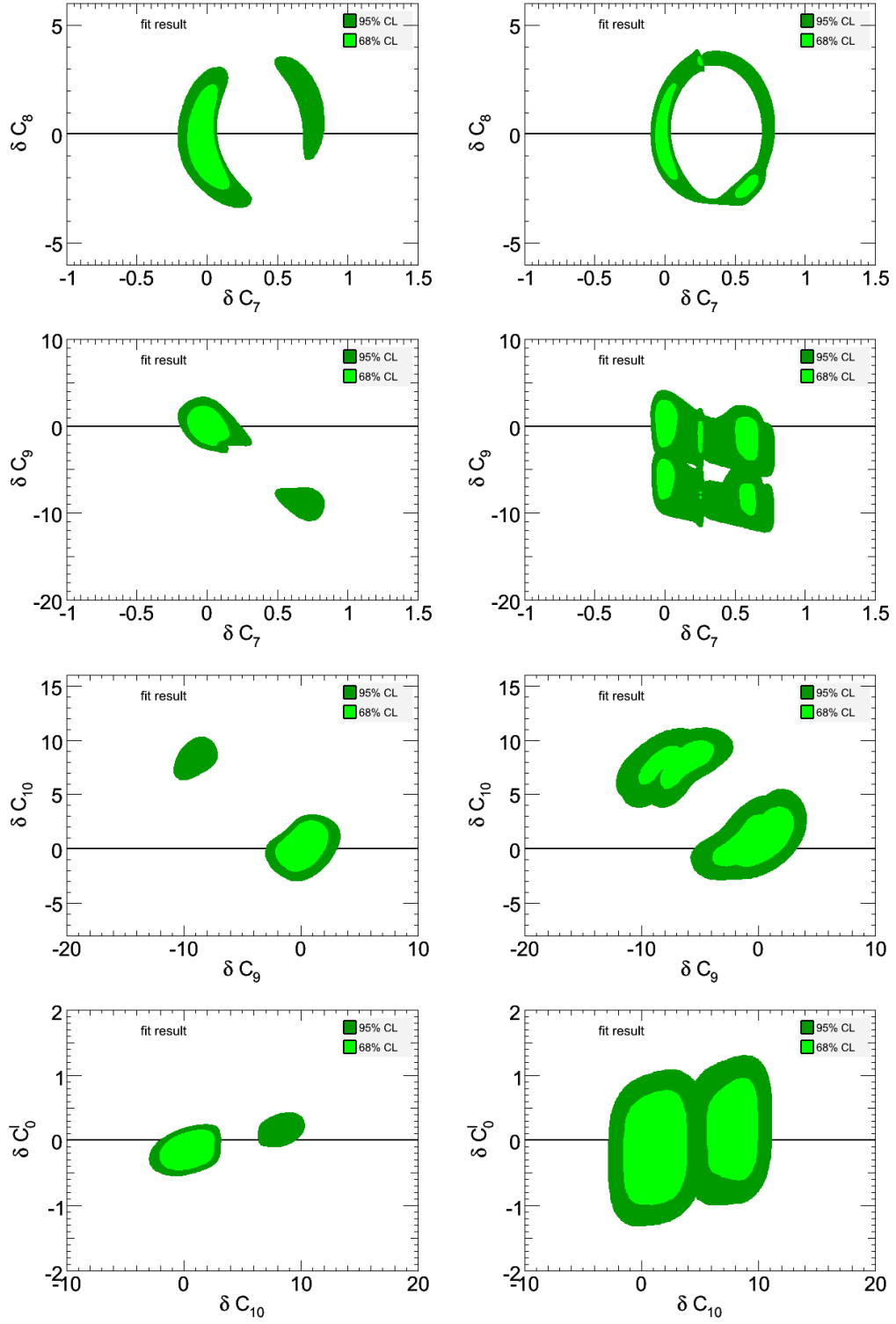


Figure 5: Global MFV fit to the various NP coefficients δC_i in the MFV effective theory *with* (left) and *without* experimental data of LHCb (right).

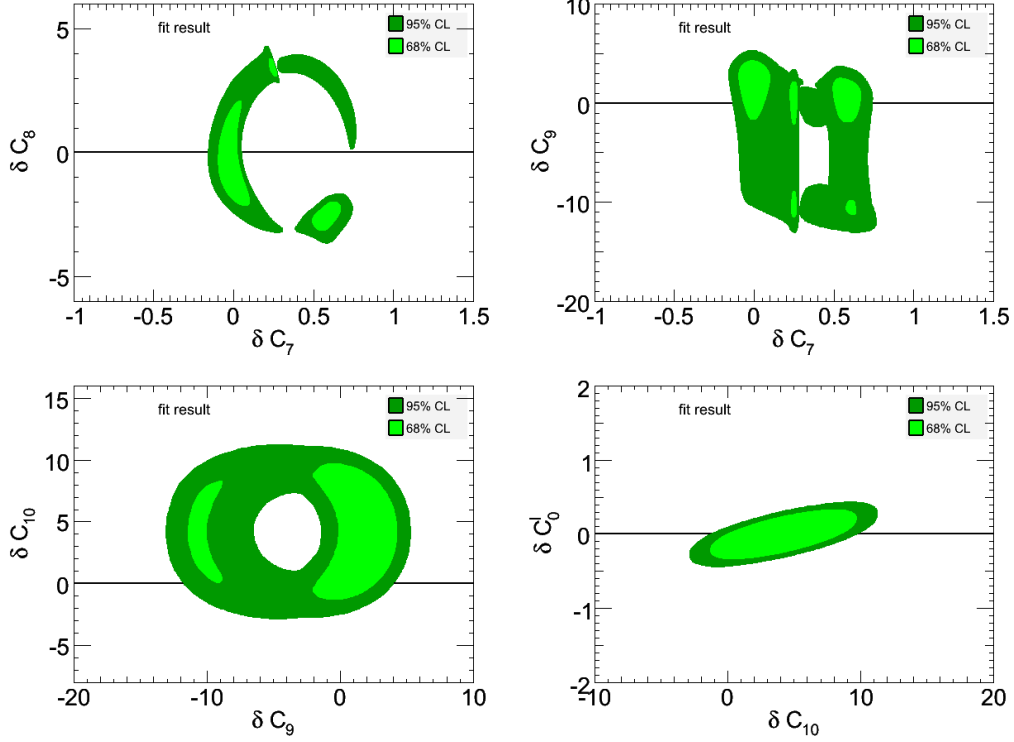


Figure 6: Global MFV fit with the latest data set *excluding* all LHCb measurements of $B \rightarrow K^* \mu^+ \mu^-$ observables.

This has to be compared with the SM prediction

$$\text{BR}(\bar{B} \rightarrow X_s \tau^+ \tau^-)_{q^2 > 14.4 \text{ GeV}^2} = (1.61 \pm 0.40) \times 10^{-7}. \quad (5.44)$$

So there are still large deviations from the SM prediction of this observable possible within the MFV scenario. And as stated above, any measurement beyond the MFV bounds would indicate the existence of new flavour structures.

- For the zero-crossing of the forward-backward asymmetry in the inclusive decay $\bar{B} \rightarrow X_s \mu^+ \mu^-$, we get the lower bound at the 95%CL

$$A_{FB}(q_0^2) = 0; \quad 1.94 \text{ GeV}^2 < q_0^2, \quad (5.45)$$

while the very precise SM prediction is $(q_0^2)^{\text{SM}} = (3.40 \pm 0.25) \text{ GeV}^2$. There is natural upper bound given by the cut due to the charm resonances. Due to the theoretical cleanliness of this observable, there are still large deviations from the SM prediction possible within the MFV benchmark. This is also true for the the complete function $A_{FB}(q^2)$.

- We have taken the measurements of the decays $\bar{B} \rightarrow X_d \gamma$ and $B_d \rightarrow \mu^+ \mu^-$ out of the global fit and find the following MFV predictions again at the 95%CL:

$$1.0 \times 10^{-5} < \text{BR}(\bar{B} \rightarrow X_d \gamma) < 4.0 \times 10^{-5}; \quad \text{BR}(B_d \rightarrow \mu^+ \mu^-) < 3.8 \times 10^{-10}. \quad (5.46)$$

The corresponding SM predictions are:

$$\text{BR}(\bar{B} \rightarrow X_d \gamma)^{\text{SM}} = (1.49 \pm 0.30) \times 10^{-5}; \quad \text{BR}(B_d \rightarrow \mu^+ \mu^-)^{\text{SM}} = (1.11 \pm 0.27) \times 10^{-10}, \quad (5.47)$$

and the present experimental data (see Table 3) is:

$$\text{BR}(\bar{B} \rightarrow X_d \gamma)^{\text{Exp.}} = (1.41 \pm 0.57) \times 10^{-5}; \quad \text{BR}(B_d \rightarrow \mu^+ \mu^-)^{\text{Exp}} < 10.0 \times 10^{-10}. \quad (5.48)$$

So the present $\bar{B} \rightarrow X_d \gamma$ measurement is already below the MFV bound and is nicely consistent with the correlation between the decays $\bar{B} \rightarrow X_s \gamma$ and $\bar{B} \rightarrow X_d \gamma$ predicted in the MFV scenario. In the case of the leptonic decay $B_d \rightarrow \mu^+ \mu^-$, however, the MFV bound is stronger than the current experimental limit. And there are still sizable deviations from the SM prediction possible within the MFV but an enhancement by orders of magnitudes due to large $\tan \beta$ effects are already ruled out by the latest measurements.

- For the large set of angular $B \rightarrow K^* \mu^+ \mu^-$ observables discussed in Section 3 we also can easily derive their MFV predictions. In an exemplary mode, we give the 95%CL MFV predictions for the $A_T^{(i)}$, averaged over the low- q^2 region ($1 \text{ GeV}^2 < q^2 < 6 \text{ GeV}^2$),

$$-0.065 < \langle A_T^{(2)} \rangle < -0.022; \quad 0.34 < \langle A_T^{(3)} \rangle < 0.99; \quad 0.19 < \langle A_T^{(4)} \rangle < 1.27, \quad (5.49)$$

and for the $H_T^{(i)}$, averaged over the high- q^2 region ($14.18 \text{ GeV}^2 < q^2 < 16 \text{ GeV}^2$),

$$\langle H_T^{(1)} \rangle = 1, \quad -1.01 < \langle H_T^{(2)} \rangle < -0.44, \quad -1.01 < \langle H_T^{(3)} \rangle < -0.44. \quad (5.50)$$

Due to the experimental and theoretical uncertainties of the $A_T^{(i)}$ observables, discussed in Refs. [55] or [63], the predicted MFV range cannot be really separated from the SM prediction; any significant deviation from the SM prediction indicates new flavour structures. But for the $H_T^{(i)}$ observables deviations from the SM are still possible within the MFV scenario.

- For the rare $s \rightarrow d$ transitions we refer again to the previous analysis in Ref. [15]. We just state that the existing rather weak experimental bound on the branching ratio of $\text{BR}(K^+ \rightarrow \pi^+ \nu \bar{\nu})$ [89] implies MFV predictions for the flavour observables $\text{BR}(B \rightarrow K^{(*)} \nu \bar{\nu})$ and $\text{BR}(K_L \rightarrow \pi^0 \nu \bar{\nu})$. Moreover, as in the case of the two decays $B_{s,d} \rightarrow \mu \mu$, the charged and neutral $K \rightarrow \pi \nu \bar{\nu}$ decays are governed by only one parameter, namely the real coefficient $\delta C_{\nu \bar{\nu}}$ in the MFV effective theory (see Eq.(2.9)), thus, the ratio of the two $K \rightarrow \pi \nu \bar{\nu}$ allows for an important model-independent test of the MFV hypothesis. There will be two dedicated kaon experiments, E-14 Koto at J-PARC [90] and Na42 at CERN [91], for this task in the near future.

Acknowledgement

TH thanks the CERN theory group for its hospitality during his regular visits to CERN where part of this work was written

A Effective, new, and modified Wilson coefficients

The standard effective Wilson coefficients are defined as follows:

$$C_i^{\text{eff}}(\mu) = C_i(\mu), \text{ for } i = 1, \dots, 6, \quad C_7^{\text{eff}}(\mu) = C_7(\mu) + \sum_{j=1}^6 y_j C_j(\mu), \quad C_8^{\text{eff}}(\mu) = C_8(\mu) + \sum_{j=1}^6 z_j C_j(\mu). \quad (\text{A.1})$$

In the $\overline{\text{MS}}$ scheme, one fixes $\vec{y} = (0, 0, -\frac{1}{3}, -\frac{4}{9}, -\frac{20}{3}, -\frac{80}{9})$ and $\vec{z} = (0, 0, 1, -\frac{1}{6}, 20, -\frac{10}{3})$, then the leading-order $b \rightarrow s\gamma$ and $b \rightarrow sg$ matrix elements of the effective Hamiltonian are proportional to the leading-order terms in C_7^{eff} and C_8^{eff} [44]. Moreover, we have $C_{10}^{\text{eff}} = C_{10}(\mu)$, and C_9^{eff} is defined as:

$$\begin{aligned}
C_9^{\text{eff}}(s) &= C_9(\mu) + \sum_{i=1}^6 C_i(\mu) \gamma_{i9}^{(0)} \ln\left(\frac{m_b}{\mu}\right) + \frac{4}{3}C_3(\mu) + \frac{64}{9}C_5(\mu) + \frac{64}{27}C_6(\mu) \\
&+ g(\hat{m}_c, s) \left(\frac{4}{3}C_1(\mu) + C_2(\mu) + 6C_3(\mu) + 60C_5(\mu) \right) \\
&+ g(1, s) \left(-\frac{7}{2}C_3(\mu) - \frac{2}{3}C_4(\mu) - 38C_5(\mu) - \frac{32}{3}C_6(\mu) \right) \\
&+ g(0, s) \left(-\frac{1}{2}C_3(\mu) - \frac{2}{3}C_4(\mu) - 8C_5(\mu) - \frac{32}{3}C_6(\mu) \right)
\end{aligned} \tag{A.2}$$

where the function $g(\hat{m}_c, s)$ is given as

$$\begin{aligned}
g(z, s) &= -\frac{4}{9} \ln(z) + \frac{8}{27} + \frac{16}{9} \frac{z}{s} - \frac{2}{9} \left(2 + \frac{4z}{s} \right) \sqrt{\left| \frac{4z-s}{s} \right|} \times \\
&\times \begin{cases} 2 \arctan \sqrt{\frac{s}{4z-s}} & \text{for } s < 4z, \\ \ln \left(\frac{\sqrt{s} + \sqrt{s-4z}}{\sqrt{s} - \sqrt{s-4z}} \right) - i\pi & \text{for } s > 4z. \end{cases}
\end{aligned} \tag{A.3}$$

The new Wilson coefficients are introduced in Ref. [49] and are defined as:

$$C_7^{\text{new}}(s) = \left(1 + \frac{\alpha_s}{\pi} \sigma_7(s) \right) C_7^{\text{eff}} - \frac{\alpha_s}{4\pi} \left[C_1^{(0)} F_1^{(7)}(s) + C_2^{(0)} F_2^{(7)}(s) + C_8^{\text{eff}(0)} F_8^{(7)}(s) \right], \tag{A.4}$$

$$C_9^{\text{new}}(s) = \left(1 + \frac{\alpha_s}{\pi} \sigma_9(s) \right) C_9^{\text{eff}}(s) - \frac{\alpha_s}{4\pi} \left[C_1^{(0)} F_1^{(9)}(s) + C_2^{(0)} F_2^{(9)}(s) + C_8^{\text{eff}(0)} F_8^{(9)}(s) \right], \tag{A.5}$$

$$C_{10}^{\text{new}}(s) = \left(1 + \frac{\alpha_s}{\pi} \sigma_9(s) \right) C_{10}^{\text{eff}}. \tag{A.6}$$

The virtual corrections to $O_{1,2}$ and O_8 are embedded in $F_{1,2}^{(7,9)}$ and $F_8^{(7,9)}$. The σ_i functions indicate certain bremsstrahlung contributions (see Ref. [49]).

Finally, the modified effective Wilson coefficients introduced in Ref. [18] include contributions of the four-quark operators but also of the gluon dipole operators. It is important to note that these

	r_1	r_2	$m_R^2 [\text{GeV}^2]$	$m_{fit}^2 [\text{GeV}^2]$
V	0.923	-0.511	5.32^2	49.40
A_1		0.290		40.38
A_2	-0.084	0.342		52.00

Table 6: Fit parameters describing the q^2 dependence of the form factors V and $A_{1,2}$ in the LCSR approach [73].

quantities are different from *the effective Wilson coefficients* $C_{7,9}^{\text{eff}}$ introduced before.

$$C_9^{\text{eff,mod}} = C_9 + h(0, q^2) \left[\frac{4}{3} C_1 + C_2 + \frac{11}{2} C_3 - \frac{2}{3} C_4 + 52 C_5 - \frac{32}{3} C_6 \right] \quad (\text{A.7})$$

$$- \frac{1}{2} h(m_b, q^2) \left[7 C_3 + \frac{4}{3} C_4 + 76 C_5 + \frac{64}{3} C_6 \right] + \frac{4}{3} \left[C_3 + \frac{16}{3} C_5 + \frac{16}{9} C_6 \right]$$

$$+ \frac{\alpha_s}{4\pi} \left[C_1 (B(q^2) + 4C(q^2)) - 3C_2 (2B(q^2) - C(q^2)) - C_8 F_8^{(9)}(q^2) \right]$$

$$+ 8 \frac{m_c^2}{q^2} \left[\frac{4}{9} C_1 + \frac{1}{3} C_2 + 2C_3 + 20C_5 \right],$$

$$C_7^{\text{eff,mod}} = C_7 - \frac{1}{3} \left[C_3 + \frac{4}{3} C_4 + 20C_5 + \frac{80}{3} C_6 \right] + \frac{\alpha_s}{4\pi} \left[(C_1 - 6C_2) A(q^2) - C_8 F_8^{(7)}(q^2) \right], \quad (\text{A.8})$$

The functions A, B, C and $F_8^{(7)}, F_8^{(9)}$ are given in Refs. [92] and [16].

B Determination of the soft form factors

To obtain the soft $B \rightarrow K^*$ form factors we have used the following factorization scheme [17]:

$$\xi_{\perp}(q^2) = \frac{M_B}{M_B + m_{K^*}} V(q^2), \quad (\text{B.1})$$

$$\xi_{\parallel}(q^2) = \frac{M_B + m_{K^*}}{2E_{K^*}} A_1(q^2) - \frac{M_B - m_{K^*}}{M_B} A_2(q^2). \quad (\text{B.2})$$

The full form factors V and $A_{1,2}$ have been taken from light-cone sum rule (LCSR) calculations [73]:

$$V(q^2) = \frac{r_1}{1 - q^2/m_R^2} + \frac{r_2}{1 - q^2/m_{fit}^2}, \quad (\text{B.3})$$

$$A_1(q^2) = \frac{r_2}{1 - q^2/m_{fit}^2}, \quad (\text{B.4})$$

$$A_2(q^2) = \frac{r_1}{1 - q^2/m_{fit}^2} + \frac{r_2}{(1 - q^2/m_{fit}^2)^2}, \quad (\text{B.5})$$

where the fit parameters $r_{1,2}, m_R^2$ and m_{fit}^2 are given in Table 6.

References

- [1] Belle collaboration: <http://belle.kek.jp/>
- [2] BaBar collaboration: <http://www.slac.stanford.edu/BFROOT/>
- [3] CDF collaboration: <http://www-cdf.fnal.gov/physics/new/bottom/bottom.html>
- [4] D0 collaboration: <http://www-d0.fnal.gov/Run2Physics/WWW/results/b.htm>
- [5] LHCb collaboration: <http://lhcb.web.cern.ch/lhcb/>
- [6] M. Kobayashi and T. Maskawa, *Prog. Theor. Phys.* **49** (1973) 652.
- [7] N. Cabibbo, *Phys. Rev. Lett.* **10** (1963) 531.
- [8] T. Hurth and M. Nakao, *Ann. Rev. Nucl. Part. Sci.* **60** (2010) 645 [arXiv:1005.1224 [hep-ph]].
- [9] T. Hurth, *Rev. Mod. Phys.* **75** (2003) 1159 [hep-ph/0212304].
- [10] F. Mahmoudi, arXiv:1205.3099 [hep-ph].
- [11] T. Hurth and S. Kraml, *AIP Conf. Proc.* **1441** (2012) 713 [arXiv:1110.3804 [hep-ph]].
- [12] R. S. Chivukula and H. Georgi, *Phys. Lett. B* **188** (1987) 99.
- [13] L. J. Hall and L. Randall, *Phys. Rev. Lett.* **65**, 2939 (1990).
- [14] G. D'Ambrosio, G. F. Giudice, G. Isidori and A. Strumia, *Nucl. Phys. B* **645** (2002) 155 [hep-ph/0207036].
- [15] T. Hurth, G. Isidori, J. F. Kamenik and F. Mescia, *Nucl. Phys. B* **808** (2009) 326 [arXiv:0807.5039 [hep-ph]].
- [16] M. Beneke, T. Feldmann and D. Seidel, *Nucl. Phys. B* **612** (2001) 25 [hep-ph/0106067].
- [17] M. Beneke, T. Feldmann and D. Seidel, *Eur. Phys. J. C* **41** (2005) 173 [hep-ph/0412400].
- [18] B. Grinstein and D. Pirjol, *Phys. Rev. D* **70** (2004) 114005 [hep-ph/0404250].
- [19] M. Beylich, G. Buchalla and T. Feldmann, *Eur. Phys. J. C* **71** (2011) 1635 [arXiv:1101.5118 [hep-ph]].
- [20] M. Bona *et al.* [UTfit Collaboration], *JHEP* **0603** (2006) 080 [hep-ph/0509219].
- [21] A. Lenz, U. Nierste, J. Charles, S. Descotes-Genon, A. Jantsch, C. Kaufhold, H. Lacker and S. Monteil *et al.*, *Phys. Rev. D* **83** (2011) 036004 [arXiv:1008.1593 [hep-ph]].
- [22] A. Lenz, U. Nierste, J. Charles, S. Descotes-Genon, H. Lacker, S. Monteil, V. Niess and S. T'Jampens, arXiv:1203.0238 [hep-ph].
- [23] L. Mercolli and C. Smith, *Nucl. Phys. B* **817** (2009) 1 [arXiv:0902.1949 [hep-ph]].
- [24] P. Paradisi and D. M. Straub, *Phys. Lett. B* **684** (2010) 147 [arXiv:0906.4551 [hep-ph]].
- [25] T. Feldmann and T. Mannel, hep-ph/0611095.

- [26] K. Agashe, M. Papucci, G. Perez and D. Pirjol, hep-ph/0509117.
- [27] B. Grinstein, V. Cirigliano, G. Isidori and M. B. Wise, hep-ph/0608123.
- [28] E. Nikolidakis and C. Smith, Phys. Rev. D **77** (2008) 015021 [arXiv:0710.3129 [hep-ph]].
- [29] C. Csaki, Y. Grossman and B. Heidenreich, Phys. Rev. D **85**, 095009 (2012) [arXiv:1111.1239 [hep-ph]].
- [30] P. Paradisi, M. Ratz, R. Schieren and C. Simonetto, Phys. Lett. B **668** (2008) 202 [arXiv:0805.3989 [hep-ph]].
- [31] G. Colangelo, E. Nikolidakis and C. Smith, Eur. Phys. J. C **59** (2009) 75 [arXiv:0807.0801 [hep-ph]].
- [32] G. Isidori and D. M. Straub, arXiv:1202.0464 [hep-ph].
- [33] E. Nikolidakis and C. Smith, Phys. Rev. D **77** (2008) 015021 [arXiv:0710.3129 [hep-ph]].
- [34] C. Csaki, Y. Grossman and B. Heidenreich, Phys. Rev. D **85**, 095009 (2012) [arXiv:1111.1239 [hep-ph]].
- [35] M. Antonelli *et al.* [FlaviaNet Working Group on Kaon Decays], arXiv:0801.1817 [hep-ph] and online update at <http://www.lnf.infn.it/wg/vus/> from Rare K decays and Decay Constants.
- [36] J. Brod and M. Gorbahn, arXiv:0805.4119 [hep-ph].
- [37] A. J. Buras, M. Gorbahn, U. Haisch and U. Nierste, JHEP **0611**, 002 (2006) [arXiv:hep-ph/0603079];
- [38] F. Mescia and C. Smith, Phys. Rev. D **76**, 034017 (2007) [arXiv:0705.2025 [hep-ph]].
- [39] A. Czarnecki and W. J. Marciano, Phys. Rev. Lett. **81** (1998) 277 [hep-ph/9804252].
- [40] M. Misiak, H. M. Asatrian, K. Bieri, M. Czakon, A. Czarnecki, T. Ewerth, A. Ferroglia and P. Gambino *et al.*, Phys. Rev. Lett. **98** (2007) 022002 [hep-ph/0609232].
- [41] P. Gambino and P. Giordano, Phys. Lett. B **669** (2008) 69 [arXiv:0805.0271 [hep-ph]].
- [42] M. Benzke, S. J. Lee, M. Neubert and G. Paz, JHEP **1008** (2010) 099 [arXiv:1003.5012 [hep-ph]].
- [43] M. Misiak, arXiv:0808.3134 [hep-ph].
- [44] M. Misiak and M. Steinhauser, Nucl. Phys. B **764**, 62 (2007) [arXiv:hep-ph/0609241].
- [45] T. Hurth, E. Lunghi and W. Porod, Nucl. Phys. B **704** (2005) 56 [arXiv:hep-ph/0312260].
- [46] A. L. Kagan and M. Neubert, Phys. Lett. B **539**, 227 (2002) [arXiv:hep-ph/0110078].
- [47] G. Buchalla, A. J. Buras and M. E. Lautenbacher, Rev. Mod. Phys. **68** (1996) 1125 [hep-ph/9512380].
- [48] S. W. Bosch and G. Buchalla, Nucl. Phys. B **621** (2002) 459 [hep-ph/0106081].
- [49] A. Ghinculov, T. Hurth, G. Isidori and Y. P. Yao, Nucl. Phys. B **685** (2004) 351 [hep-ph/0312128].
- [50] T. Huber, T. Hurth and E. Lunghi, Nucl. Phys. B **802** (2008) 40 [arXiv:0712.3009 [hep-ph]].

- [51] Y. Grossman, Z. Ligeti and E. Nardi, Phys. Rev. D **55** (1997) 2768 [hep-ph/9607473].
- [52] Z. -h. Xiong and J. M. Yang, Nucl. Phys. B **602** (2001) 289 [hep-ph/0012217].
- [53] Z. Xiong and J. M. Yang, Nucl. Phys. B **628** (2002) 193 [hep-ph/0105260].
- [54] Z. Ligeti and F. J. Tackmann, Phys. Lett. B **653** (2007) 404 [arXiv:0707.1694v2].
- [55] U. Egede, T. Hurth, J. Matias, M. Ramon and W. Reece, JHEP **0811** (2008) 032 [arXiv:0807.2589 [hep-ph]].
- [56] F. Kruger and J. Matias, Phys. Rev. D **71** (2005) 094009 [hep-ph/0502060]. .
- [57] F. Kruger, L. M. Sehgal, N. Sinha and R. Sinha, Phys. Rev. D **61** (2000) 114028 [Erratum-ibid. D **63** (2001) 019901] [hep-ph/9907386].
- [58] W. Altmannshofer, P. Ball, A. Bharucha, A. J. Buras, D. M. Straub and M. Wick, JHEP **0901** (2009) 019 [arXiv:0811.1214 [hep-ph]].
- [59] U. Egede, T. Hurth, J. Matias, M. Ramon and W. Reece, JHEP **1010** (2010) 056 [arXiv:1005.0571 [hep-ph]].
- [60] C. Bobeth, G. Hiller and G. Piranishvili, JHEP **0807** (2008) 106 [arXiv:0805.2525 [hep-ph]].
- [61] C. Bobeth, G. Hiller and D. van Dyk, JHEP **1007** (2010) 098 [arXiv:1006.5013 [hep-ph]].
- [62] C. Bobeth, G. Hiller and D. van Dyk, JHEP **1107** (2011) 067 [arXiv:1105.0376 [hep-ph]].
- [63] F. Beaujean, C. Bobeth, D. van Dyk and C. Wacker, arXiv:1205.1838 [hep-ph].
- [64] J. Charles, A. Le Yaouanc, L. Oliver, O. Pene and J. C. Raynal, Phys. Rev. D **60** (1999) 014001 [hep-ph/9812358].
- [65] P. Dimopoulos *et al.* [ETM Collaboration], *Lattice QCD determination of m_b , f_B and f_{B_s} with twisted mass Wilson fermions*, JHEP **1201** (2012) 046 [arXiv:1107.1441].
- [66] A. Bazavov *et al.* [Fermilab Lattice and MILC Collaboration], *B- and D-meson decay constants from three-flavor lattice QCD*, arXiv:1112.3051 [hep-lat].
- [67] E. T. Neil *et al.* [for the Fermilab Lattice and for the MILC Collaborations], *B and D meson decay constants from 2+1 flavor improved staggered simulations*, arXiv:1112.3978 [hep-lat].
- [68] H. Na, C. J. Monahan, C. T. H. Davies, R. Horgan, G. P. Lepage and J. Shigemitsu, *The B and B_s Meson Decay Constants from Lattice QCD*, arXiv:1202.4914 [hep-lat].
- [69] C. McNeile, C. T. H. Davies, E. Follana, K. Hornbostel and G. P. Lepage, *High-Precision f_{B_s} and HQET from Relativistic Lattice QCD*, Phys. Rev. D **85** (2012) 031503 [arXiv:1110.4510].
- [70] C. Davies, *Standard Model Heavy Flavor physics on the Lattice*, arXiv:1203.3862 [hep-lat].
- [71] K. Nakamura *et al.* [Particle Data Group], *Review of particle physics*, J. Phys. G **37** (2010) 075021 and 2011 partial update for the 2012 edition.
- [72] P. Ball, V. M. Braun and A. Lenz, *Twist-4 distribution amplitudes of the K^* and ϕ mesons in QCD*, JHEP **0708** (2007) 090 [arXiv:0707.1201].

- [73] P. Ball and R. Zwicky, $B_{d,s} \rightarrow \rho, \omega, K^*, \phi$ decay form-factors from light-cone sum rules revisited, Phys. Rev. D **71** (2005) 014029 [hep-ph/0412079].
- [74] P. Ball and R. Zwicky, $|V_{td}/V_{ts}|$ from $B \rightarrow V\gamma$, JHEP **0604** (2006) 046 [hep-ph/0603232].
- [75] F. Mahmoudi, *SuperIso: A Program for calculating the isospin asymmetry of $B \rightarrow K^*\gamma$ in the MSSM*, Comput. Phys. Commun. **178** (2008) 745 [arXiv:0710.2067].
- [76] F. Mahmoudi, *SuperIso v2.3: A Program for calculating flavor physics observables in Supersymmetry*, Comput. Phys. Commun. **180** (2009) 1579 [arXiv:0808.3144].
- [77] D. Asner *et al.* [Heavy Flavor Averaging Group Collaboration], arXiv:1010.1589 [hep-ex] and online updates at <http://www.slac.stanford.edu/xorg/hfag>.
- [78] P. del Amo Sanchez *et al.* [BABAR Collaboration], Phys. Rev. D **82** (2010) 051101 [arXiv:1005.4087 [hep-ex]].
- [79] W. Wang, arXiv:1102.1925 [hep-ex].
- [80] R. Aaij *et al.* [LHCb Collaboration], *Strong constraints on the rare decays $B_s \rightarrow \mu^+\mu^-$ and $B^0 \rightarrow \mu^+\mu^-$* , arXiv:1203.4493 [hep-ex].
- [81] [LHCb Collaboration], *Differential branching fraction and angular analysis of the $B^0 \rightarrow K^*\mu^+\mu^-$ decay* LHCb-CONF-2012-008, presented at the 47th Rencontres de Moriond on QCD and High Energy Interactions.
- [82] B. Aubert *et al.* [BABAR Collaboration], Phys. Rev. Lett. **93** (2004) 081802 [hep-ex/0404006].
- [83] M. Iwasaki *et al.* [Belle Collaboration], Phys. Rev. D **72** (2005) 092005 [hep-ex/0503044].
- [84] T. Aaltonen *et al.* [CDF Collaboration], Phys. Rev. Lett. **100** (2008) 101802 [arXiv:0712.1708 [hep-ex]].
- [85] CDF Collaboration, CDF note 10047.
- [86] F. Mahmoudi, S. Neshatpour and J. Orloff, arXiv:1205.1845 [hep-ph].
- [87] K. de Bruyn, R. Fleischer, R. Knegjens, P. Koppenburg, M. Merk and N. Tuning, arXiv:1204.1735 [hep-ph].
- [88] K. de Bruyn, R. Fleischer, R. Knegjens, P. Koppenburg, M. Merk, A. Pellegrino and N. Tuning, arXiv:1204.1737 [hep-ph].
- [89] S. Adler *et al.* [E787 Collaboration], Phys. Rev. D **77** (2008) 052003;
- [90] <http://koto.kek.jp/>
- [91] <http://na62.web.cern.ch/na62/>
- [92] D. Seidel, Phys. Rev. D **70** (2004) 094038 [hep-ph/0403185].